

Final State Rescattering and Color-suppressed $\bar{B}^0 \rightarrow D^{(*)0}h^0$ Decays

Chun-Khiang Chua and Wei-Shu Hou

Physics Department, National Taiwan University, Taipei, Taiwan 10764, Republic of China

Kwei-Chou Yang

Physics Department, Chung Yuan Christian University, Chung-Li, Taiwan 32023, Republic of China

(Dated: October 24, 2018)

The color-suppressed $\bar{B}^0 \rightarrow D^{(*)0}\pi^0$, $D^{(*)0}\eta$, $D^0\omega$ decay modes have just been observed for the first time. The rates are all larger than expected, hinting at the presence of final state interactions. Considering $\bar{B}^0 \rightarrow D^{(*)0}\pi^0$ mode alone, an elastic $D^{(*)}\pi \rightarrow D^{(*)}\pi$ rescattering phase difference $\delta \equiv \delta_{1/2} - \delta_{3/2} \sim 30^\circ$ would suffice, but the $\bar{B}^0 \rightarrow D^{(*)0}\eta$, $D^0\omega$ modes compel one to extend the elastic formalism to SU(3) symmetry. We find that a universal $a_2/a_1 = 0.25$ and two strong phase differences $20^\circ \sim \theta < \delta < \delta' \sim 50^\circ$ can describe both DP and D^*P modes rather well; the large phase of order 50° is needed to account for the strength of *both* the $D^{(*)0}\pi^0$ and $D^{(*)0}\eta$ modes. For DV modes, the nonet symmetry reduces the number of physical phases to just one, giving better predictive power. Two solutions are found. We predict the rates of the $\bar{B}^0 \rightarrow D_s^+K^-$, $D_s^{*+}K^-$, $D^0\rho^0$, $D_s^+K^{*-}$ and $D^0\phi$ modes, as well as $\bar{B}^0 \rightarrow D^0\bar{K}^0$, $D^{*0}\bar{K}^0$, $D^0\bar{K}^{*0}$ modes. The formalism may have implications for rates and CP asymmetries of charmless modes.

PACS numbers: 11.30.Hv, 13.25.Hw, 14.40.Nd

I. INTRODUCTION

The Belle Collaboration has recently observed [1] the $\bar{B}^0 \rightarrow D^0\pi^0$, $D^{*0}\pi^0$, $D^0\eta$ and $D^0\omega$ decay modes, as well as finding evidence for $\bar{B}^0 \rightarrow D^{*0}\eta$ and $D^{*0}\omega$. The decay branching ratios (\mathcal{B}) are all at a few times 10^{-4} level:

$$\begin{aligned} \mathcal{B}(\bar{B}^0 \rightarrow D^0\pi^0) &= (3.1 \pm 0.4 \pm 0.5) \times 10^{-4}, \\ \mathcal{B}(\bar{B}^0 \rightarrow D^{*0}\pi^0) &= (2.7^{+0.8}_{-0.7}{}^{+0.5}_{-0.6}) \times 10^{-4}, \\ \mathcal{B}(\bar{B}^0 \rightarrow D^0\eta) &= (1.4^{+0.5}_{-0.4} \pm 0.3) \times 10^{-4}, \\ \mathcal{B}(\bar{B}^0 \rightarrow D^0\omega) &= (1.8 \pm 0.5^{+0.4}_{-0.3}) \times 10^{-4}, \\ \mathcal{B}(\bar{B}^0 \rightarrow D^{*0}\eta) &= (2.0^{+0.9}_{-0.8} \pm 0.4) \times 10^{-4}, \\ \mathcal{B}(\bar{B}^0 \rightarrow D^{*0}\omega) &= (3.1^{+1.3}_{-1.1} \pm 0.8) \times 10^{-4}. \end{aligned}$$

The CLEO Collaboration has also reported [2] the observation of $\bar{B}^0 \rightarrow D^0\pi^0$, $D^{*0}\pi^0$ modes,

$$\begin{aligned} \mathcal{B}(\bar{B}^0 \rightarrow D^0\pi^0) &= (2.74^{+0.36}_{-0.32} \pm 0.55) \times 10^{-4}, \\ \mathcal{B}(\bar{B}^0 \rightarrow D^{*0}\pi^0) &= (2.20^{+0.59}_{-0.52} \pm 0.79) \times 10^{-4}, \end{aligned}$$

with rates in agreement with Belle. These modes are usually called color-suppressed B decays. In contrast to the much faster “color-allowed” $\bar{B}^0 \rightarrow D^+\pi^-$ ($\mathcal{B} \simeq 3 \times 10^{-3}$ [3]) decay where π^- is emitted by the charged current (Fig. 1(a)), there is a color mismatch in forming the D^0 meson from c and \bar{u} produced by $b \rightarrow c\bar{u}d$ decay (Fig. 1(b)). We have indicated in Figs. 1(a) and (b) the effective Wilson coefficients, a_1 and a_2 [4], that is responsible for the decay. For the charged $B^- \rightarrow D^0\pi^-$ decay, both a_1 and a_2 type of diagrams contribute.

The factorization of the $\bar{B}^0 \rightarrow D^+\pi^-$ decay amplitude has recently been demonstrated to follow from QCD in the heavy b quark limit [5, 6], and a_1 as computed from QCD factorization is close to $a_1^{(\text{eff})} \sim 1-1.1$ from “generalized factorization” [4]. On the other hand, it is known

that the effective coefficient $a_2^{(\text{eff})}$ cannot be calculated in QCD factorization [5]. It is remarkable that the $a_2^{(\text{eff})}$ value as extracted from the celebrated $\bar{B} \rightarrow J/\psi\bar{K}^{(*)}$ modes agrees rather well with the value extracted from $B^- \rightarrow D^0\pi^-$, i.e. consistent with $a_2^{(\text{eff})} \simeq 0.2-0.3$ and real. However, the $D^{(*)0}\pi^0$ rates as observed by Belle and CLEO are considerably higher than the generalized factorization estimates [4] using this $a_2^{(\text{eff})}$ value, suggesting that final state rescatterings (FSI) such as $D^{(*)+}\pi^- \rightarrow D^{(*)0}\pi^0$ could be active. Alternatively, it could indicate non-universal a_2 , that is, a_2 for color-suppressed modes are larger than [7] a_2 for $J/\psi\bar{K}^{(*)}$ modes, and are furthermore complex to accommodate $B^- \rightarrow D^{(*)0}\pi^-$. Whether in the form of FSI rescattering or a larger and complex a_2 , one in general acquires complexity of decay amplitudes in the form of CP conserving phases. This may have implications for direct CP violation asymmetries, since similar effects may be present in

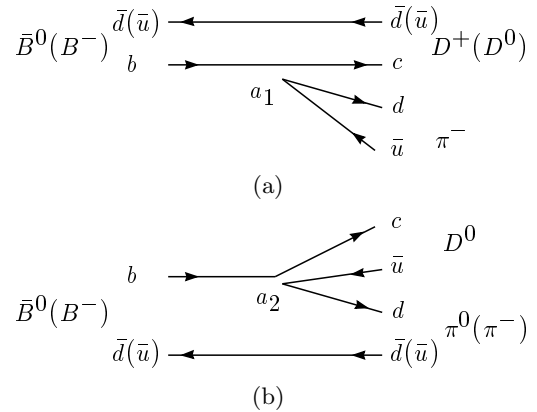


FIG. 1: Color (a) allowed and (b) suppressed $B \rightarrow D\pi$ decays.

processes such as charmless $B \rightarrow K\pi$ modes.

The experimental data in fact compels one to broaden the horizon. The Belle results on $\bar{B}^0 \rightarrow D^0\eta$ and $D^0\omega$ are considerably higher than generalized factorization estimates [4] as well, suggesting that one needs to go beyond $D\pi \rightarrow D\pi$ considerations in the FSI framework. The alternative of having process dependent a_2 's [7, 8] would imply loss of predictive power. While it is clear that a_2 in general will be process dependent, we do abhor the loss of predictive power. In this paper we wish to explore how the situation could be remedied.

Since the data is new and still rather incomplete, our approach will be phenomenological, without aim for rigor or completeness. Let us start from the isospin decomposition of $\bar{B} \rightarrow D^0\pi^-$, $D^+\pi^-$ and $D^0\pi^0$ decay amplitudes that is lucidly outlined in Ref. [4],

$$\begin{aligned} A_{D^0\pi^-} &= \sqrt{3}A_{3/2}, \\ A_{D^+\pi^-} &= \sqrt{\frac{2}{3}}A_{1/2} + \sqrt{\frac{1}{3}}A_{3/2}, \\ A_{D^0\pi^0} &= \sqrt{\frac{1}{3}}A_{1/2} - \sqrt{\frac{2}{3}}A_{3/2}, \end{aligned} \quad (1)$$

where the final state is emphasized. In the absence of FSI, the smallness of $D^0\pi^0$ rate can be viewed as due to cancellation between the $A_{1/2}$ and $A_{3/2}$ amplitudes, which are real under factorization. But these amplitudes in general become complex under FSI and $A_{D^0\pi^0}$ stands to gain strength. However, the isospin or triangular relation $A_{D^+\pi^-} = \sqrt{2}A_{D^0\pi^0} + A_{D^0\pi^-}$ always holds. We note that $A_{D^0\pi^-}$ is purely $A_{3/2}$ and can only rescatter into itself. It is therefore reasonable to maintain $a_2^{(\text{eff})}$ as extracted traditionally, i.e. the same as from $B \rightarrow J/\psi K^{(*)}$, since it is too good to be just a coincidence.

The formalism of Eq. (1) can generate $\bar{B}^0 \rightarrow D^{(*)0}\pi^0$ by *elastic* rescattering from the color-allowed $\bar{B}^0 \rightarrow D^{(*)+}\pi^-$ mode [4]. The problem is the strength of the $\bar{B}^0 \rightarrow D^{(*)0}\eta$ and $\bar{B}^0 \rightarrow D^{(*)0}\omega$ modes observed by Belle. The η and ω are isosinglets, and the η mass is quite different from pions. Thus, to generate $D^{(*)0}\eta$ and $D^{(*)0}\omega$ final states from $D^{(*)+}\pi^-$ and $D^{(*)+}\rho^-$, strictly speaking, involves *inelastic* rescattering, although only in the isospin 1/2 channel. However, it may be reasonable to extend from isospin (an excellent symmetry of the strong interaction) to SU(3), expecting that the latter becomes a good symmetry at the m_B rescattering scale.

Let us qualify the last statement further. SU(3) flavor symmetry is a symmetry of the strong interaction as QCD is flavor blind, except that the flavor symmetry is broken by quark masses. Thus, in terms of SU(3) multiplets, masses vary within the multiplet according to SU(3) breaking, and meson production differs in strength as reflected in, for example, the decay constants and transition form factors. But if we enlarge the isospin doublet $D^{(*)} = (D^{(*)+}, D^{(*)0})$ and triplet $\pi = (\pi^+, \pi^0, \pi^-)$ to SU(3) triplet $D^{(*)} = (D^{(*)+}, D^{(*)0}, D_s^{(*)+})$ and the meson octet Π (likewise from ρ to vector V), we note

that rescattering occurs at $m_B \gg m_q$ scale, hence the $\Pi \rightarrow \Pi$ strong rescattering amplitude should respect SU(3) symmetry to good degree. SU(3) breaking effects are taken into account in the initial meson formations from B meson weak decay, which is done in the (QCD) factorization framework with $a_1^{(\text{eff})}$ and $a_2^{(\text{eff})}$ as effective *short distance* Wilson coefficients.

Thus, our aim is to extend the usual *elastic* $D\pi \rightarrow D\pi$ rescattering to *quasi-elastic* $\Pi \rightarrow \Pi$ rescattering in *final state*, so $D^{(*)0}\eta$ and $D^{(*)0}\omega$ modes are naturally incorporated. Our framework is rather close in spirit to the original isospin analysis of $\bar{B} \rightarrow D\pi$, and is as close to elastic as one can get. The most general formalism involving inelastic rescatterings from all possible hadronic final states cannot be tackled. In general it involves large cancellations and, statistically speaking, small phases [9]. Hopefully, and in a sense true by duality, the inelastic effects are contained already in $a_1^{(\text{eff})}$ and $a_2^{(\text{eff})}$.

In Sec. II we introduce the general framework of a T -matrix, discuss its link to the optical theorem, and also fix the phase convention. The formalism is applied to the $\bar{B} \rightarrow D\pi$ modes in Sec. III. Three types of rescattering amplitudes are identified: a diagonal “Pomeron”-like piece, and two “Regge”-like pieces denoted as “charge-exchange” and “annihilation”. We relate these to the usual isospin 1/2 and 3/2 rescattering phases, and show that only $\delta \equiv \delta_{1/2} - \delta_{3/2}$ matters, as expected.

In Sec. IV we extend from SU(2) to SU(3) multiplets in the final state. For DP and D^*P modes, where P stands for the pseudoscalar octet, the extension is straightforward. The question of whether to include the flavor singlet η_1 in the final state is bypassed by noting a) the absence of data, which would remain the case for a while unless $\bar{B}^0 \rightarrow D^0\eta'$ turns out to be much larger than $\bar{B}^0 \rightarrow D^0\eta$, and b) $U_A(1)$ anomaly that singles out the η_1 field, and perhaps as a consequence, c) relatively small singlet-octet or $\eta-\eta'$ mixing, allowing us to identify $\eta_8 \simeq \eta$ for convenience. We thus ignore η_1 completely in this work. We find the previous picture of three types of rescattering parameters still hold, but one now has two δ -like phase differences. The extension to DV final states is treated differently. By noting that the vector mesons satisfy $U(3)$ rather than $SU(3)$ symmetry, we use a nonet V field rather than an octet one. We refrain from discussing D^*V modes since data is scarce, and since two helicity (or partial wave) amplitudes are involved.

We carry out a numerical study in Sec. V. For the DP modes, we find two sets of solutions for the two FSI phase differences, which are of order 20° and 50° . One solution is similar to the D^*P case, and has a very tiny $\bar{B}^0 \rightarrow D_s^+K^-$ decay due to the smallness of “annihilation” rescattering. The other solution gives $\mathcal{B}(\bar{B}^0 \rightarrow D_s^+K^-) \sim 5 \times 10^{-4}$, which is ruled out by experiment. For DV modes, we have two solutions: one does not have annihilation contribution hence $\mathcal{B}(\bar{B}^0 \rightarrow D^0\rho^0) \sim \mathcal{B}(\bar{B}^0 \rightarrow D^0\omega)$, while the other does not have exchange contribution and $\mathcal{B}(\bar{B}^0 \rightarrow D^0\rho^0) > \mathcal{B}(\bar{B}^0 \rightarrow D^0\omega)$.

In Sec. VI we compare our “ $a_2^{(\text{eff})}$ plus FSI rescattering” approach with the viewpoint of “process dependent a_2 ”, and discuss possible future applications. The conclusion is then offered, followed by Appendices that give same results from a SU(3) decomposition approach and a geometric (triangular) representation of our rescattering picture.

II. FINAL STATE RESCATTERING FRAMEWORK

Let H_W denote the weak decay Hamiltonian. We assume absence of weak phases (or they are factored out), hence, from time reversal invariance of $H_W (= U_T H_W^* U_T^\dagger)$, one has,

$$\langle i; \text{out} | H_W | B \rangle^* = \sum_j S_{ji}^* \langle j; \text{out} | H_W | B \rangle, \quad (2)$$

where $S_{ij} \equiv \langle i; \text{out} | j; \text{in} \rangle$ is the strong interaction S-matrix element, and we have used $U_T | \text{out} (\text{in}) \rangle^* = | \text{in} (\text{out}) \rangle$ which also fixes the phase convention. Eq. (2) can be solved by (see, for example [9])

$$\langle i; \text{out} | H_W | B \rangle = \sum_l S_{il}^{1/2} A_l^0, \quad (3)$$

where A_l^0 is a real amplitude. To show that this is indeed a solution of Eq. (2), one needs to use $S_{ij} = S_{ji}$, which follows from time reversal invariance of the strong interactions and the phase convention we have adopted. The weak decay amplitude picks up strong scattering phases [10]. Also note that since $S^{1/2}$ is unitary, we must have

$$\sum_i |\langle i; \text{out} | H_W | B \rangle|^2 = \sum_l |A_l^0|^2. \quad (4)$$

Eq. (2) implies an identity related to the optical theorem. Noting that $S = 1 + iT$, we find

$$2 \text{Im} \langle i; \text{out} | H_W | B \rangle = \sum_j T_{ji}^* \langle j; \text{out} | H_W | B \rangle. \quad (5)$$

Thus, for B decay to a two body final state with momentum (p_1, p_2) , one has the relation

$$\begin{aligned} & 2 \text{Im} M(p_B \rightarrow p_1 p_2) \\ &= \sum_j \left(\prod_{k=1}^j \int \frac{d^3 q_k}{(2\pi)^3 2E_k} \right) (2\pi)^4 \delta^4 \left(p_1 + p_2 - \sum_{k=1}^j q_k \right) \\ & \quad \times M(p_B \rightarrow \{q_k\}) M^*(p_1 p_2 \rightarrow \{q_k\}), \end{aligned} \quad (6)$$

which relates the imaginary part of the two body decay amplitude to the sum over *all possible* B decay final states $\{q_k\}$, followed by $\{q_k\} \rightarrow p_1 p_2$ rescattering. This equation is consistent with the optical theorem to all orders of the strong interactions but only to first order of the weak decay vertex, as we illustrate in Fig. 2.

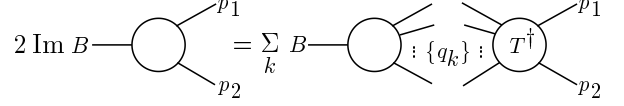


FIG. 2: Illustration of optical theorem, Eq. (6).

Before we turn to $B \rightarrow D\pi$ decay applications, let us give the isospin structure of the related amplitudes. The responsible effective weak Hamiltonian is given by

$$H_W = \frac{G_F}{\sqrt{2}} V_{cb} V_{ud}^* [c_1 \bar{d} \gamma^\mu (1 - \gamma_5) u \bar{c} \gamma_\mu (1 - \gamma_5) b + c_2 \bar{c} \gamma^\mu (1 - \gamma_5) u \bar{d} \gamma_\mu (1 - \gamma_5) b], \quad (7)$$

where $V_{cb} V_{ud}^*$ can be treated as real for our purpose. It is clear that H_W transforms like a $I = 1, I_z = 1$ vector under isospin [4]. It is useful to state explicitly the phase convention and the isospin structure of these mesons:

$$\begin{aligned} |\bar{B}^0\rangle &= |\bar{b}\bar{d}\rangle \sim \bar{b}\bar{d}|0\rangle \sim \left| \frac{1}{2}, -\frac{1}{2} \right\rangle, \\ |B^-\rangle &= |\bar{b}\bar{u}\rangle \sim \bar{b}\bar{u}|0\rangle \sim \left| \frac{1}{2}, +\frac{1}{2} \right\rangle, \\ |D^+\rangle &= |\bar{c}\bar{d}\rangle \sim \bar{c}\bar{d}|0\rangle \sim \left| \frac{1}{2}, -\frac{1}{2} \right\rangle, \\ |D^0\rangle &= |\bar{c}\bar{u}\rangle \sim \bar{c}\bar{u}|0\rangle \sim \left| \frac{1}{2}, +\frac{1}{2} \right\rangle, \\ |\pi^-\rangle &= |\bar{d}\bar{u}\rangle \sim \bar{d}\bar{u}|0\rangle \sim |1, +1\rangle, \\ |\pi^0\rangle &= \left| \frac{u\bar{u} - d\bar{d}}{\sqrt{2}} \right\rangle \sim \frac{u\bar{u} - d\bar{d}}{\sqrt{2}} |0\rangle \sim -|1, 0\rangle. \end{aligned} \quad (8)$$

Note that the isospin structure is defined according to the fields that create the states, such that they conform with the definition of the isospin structure of H_W . One could alternatively define isospin quantum numbers according to states and modify that of H_W accordingly.

By isospin decomposition, we have [4] (cf. Eq. (1)),

$$\begin{aligned} A_{D^+ \pi^-} &\equiv \langle D^+ \pi^-; \text{out} | H_W | \bar{B}^0 \rangle \\ &= \sqrt{\frac{2}{3}} A_{1/2} + \sqrt{\frac{1}{3}} A_{3/2}, \end{aligned} \quad (9)$$

$$\begin{aligned} A_{D^0 \pi^0} &\equiv \langle D^0 \pi^0; \text{out} | H_W | \bar{B}^0 \rangle \\ &= \sqrt{\frac{1}{3}} A_{1/2} - \sqrt{\frac{2}{3}} A_{3/2}, \end{aligned} \quad (10)$$

$$\begin{aligned} A_{D^0 \pi^-} &\equiv \langle D^0 \pi^-; \text{out} | H_W | B^- \rangle \\ &= \sqrt{3} A_{3/2}, \end{aligned} \quad (11)$$

where

$$\begin{aligned} A_{1/2} &= \langle (D\pi)_{1/2}; \text{out} | H_W | \bar{B}^0 \rangle, \\ A_{3/2} &= \langle (D\pi)_{3/2}; \text{out} | H_W | \bar{B}^0 \rangle \\ &= \frac{1}{\sqrt{3}} \langle (D\pi)_{3/2}; \text{out} | H_W | B^- \rangle. \end{aligned} \quad (12)$$

The last step follows from the Wigner-Eckart theorem. Eqs. (9)–(11) imply the triangular isospin relation

$$A_{D^+\pi^-} = \sqrt{2}A_{D^0\pi^0} + A_{D^0\pi^-}. \quad (13)$$

We note that the sign of $A_{D^0\pi^0}$ in Eqs. (10) and (13) is different from Ref. [4], but is consistent with Ref. [8]. It is easy to see from above equations that $|A_{1/2}|^2 + |A_{3/2}|^2 = |A_{D^+\pi^-}|^2 + |A_{D^0\pi^0}|^2$.

The isospin relations Eqs. (9)–(13) are valid whether one has (in)elastic FSI or not. For example, assuming factorization hence ignoring FSI, one has

$$\begin{aligned} A_{D^0\pi^0} &\rightarrow A_{D^0\pi^0}^f = \frac{1}{\sqrt{2}}(-C + E), \\ A_{D^0\pi^-} &\rightarrow A_{D^0\pi^-}^f = T + C, \\ A_{D^+\pi^-} &\rightarrow A_{D^+\pi^-}^f = T + E, \end{aligned} \quad (14)$$

where T, C, E are the color-allowed external W -emission, color-suppressed internal W -emission and W -exchange amplitudes, which we shall discuss later. These amplitudes clearly satisfy Eq. (13).

The general validity of Eqs. (9)–(13) in fact allows one to extract $A_{1/2}$ and $A_{3/2}$ directly from the measured $D^{(*)}\pi$ rates without any further recourse to theory. Using the Belle and CLEO average of $\mathcal{B}(\overline{B}^0 \rightarrow D^0\pi^0) = (2.9 \pm 0.5) \times 10^{-4}$ and $\mathcal{B}(\overline{B}^0 \rightarrow D^{*0}\pi^0) = (2.5 \pm 0.7) \times 10^{-4}$, with other rates and $\tau(B^+)/\tau(B^0) = 1.073 \pm 0.027$ taken from PDG [3], we find

$$\begin{aligned} \frac{|A_{1/2}|^{\text{expt.}}}{\sqrt{2}|A_{3/2}|^{\text{expt.}}} &= 0.71 \pm 0.11 \quad (0.75 \pm 0.08), \\ |\delta|^{\text{expt.}} &= 29^\circ \pm 6^\circ \quad (30^\circ \pm 7^\circ), \end{aligned} \quad (15)$$

for $D^{(*)}\pi$ modes, where $\delta \equiv \delta_{1/2} - \delta_{3/2}$ is the phase difference between $A_{1/2}$ and $A_{3/2}$. This strongly suggests the presence of FSI [7, 8, 11].

As we turn on FSI, although the isospin relations still hold, we would clearly lose control if the full structure shown in Eq. (6) is employed. Even if all possible B decay rates can be measured, it would be impossible to know the phases of each amplitude. Furthermore, we know very little about the strong rescattering amplitudes. However, the subset of two body final states that may be reached via *elastic* rescatterings stand out compared to inelastic channels. It has been shown from duality arguments [12] as well as a statistical approach [9] that inelastic FSI amplitudes tend to cancel each other and lead to small FSI phases. We shall therefore separate $\{q_k\}$ into two body elastic channels plus the rest. We first explore the familiar [4] $\overline{B} \rightarrow D^+\pi^-, D^0\pi^-$ and $D^0\pi^0$ case, then try to stretch the scope of elasticity.

III. ELASTIC FSI IN THE $D\pi$ SYSTEM

Let us consider elastic final state rescattering in $\overline{B} \rightarrow D\pi$ modes. By using Eq. (3), with A_l^0 taken as the

factorization amplitudes of Eq. (14), one has

$$\begin{pmatrix} A_{D^0\pi^-} \\ A_{D^+\pi^-} \\ A_{D^0\pi^0} \end{pmatrix} = \mathcal{S}^{1/2} \begin{pmatrix} A_{D^0\pi^-}^f \\ A_{D^+\pi^-}^f \\ A_{D^0\pi^0}^f \end{pmatrix}. \quad (16)$$

A major assumption is involved here: we assume that one can separate hard and soft effects. The factorization amplitudes sum over “hard” contributions, including attempts at incorporating the effects of the largely intractable full set (generalized to n body) of inelastic amplitudes, illustrated for two body final state in Fig. 2. The $\mathcal{S}^{1/2}$ matrix describes the nonperturbative FSI from the factorized $D\pi$ “source” amplitudes. We illustrate this in Fig. 3, where the “hard” part is shrunk to a point, and we focus on two body elastic FSI.

It is instructive to show how $\mathcal{S}^{1/2}$ can be obtained. In the usual approach, one notes that with only elastic $D\pi \rightarrow D\pi$ rescatterings, the S-matrix is diagonal in the isospin basis (isospin invariance), that is

$$\mathcal{S}_{\text{diag}} = U \mathcal{S} U^T = \text{diag}(S_{\frac{3}{2}, \frac{3}{2}}, S_{\frac{3}{2}, \frac{1}{2}}, S_{\frac{1}{2}, \frac{1}{2}}), \quad (17)$$

$$U = \begin{pmatrix} 1 & 0 & 0 \\ 0 & \sqrt{\frac{1}{3}} & -\sqrt{\frac{2}{3}} \\ 0 & \sqrt{\frac{2}{3}} & \sqrt{\frac{1}{3}} \end{pmatrix}. \quad (18)$$

Unitarity then implies that the diagonal elements of \mathcal{S} can only be pure phases, or

$$S_{\frac{1}{2}, \frac{1}{2}} = e^{2i\delta_{1/2}}, \quad S_{\frac{3}{2}, \frac{3}{2}} = e^{2i\delta_{3/2}}. \quad (19)$$

$\mathcal{S}^{1/2}$ is likewise diagonal, i.e. $(\mathcal{S}^{1/2})_{1/2, 1/2} = e^{i\delta_{1/2}}$ and $(\mathcal{S}^{1/2})_{3/2, 3/2} = e^{i\delta_{3/2}}$. Elastic FSI is equivalent to $A_I = e^{i\delta_I} |A_I^f|$ with $|A_I^f|$ taken from factorization approach [4]. The isospin relation of Eq. (13) is clearly satisfied.

For later use we express $\mathcal{S}^{1/2}$ in the basis of Eq. (16),

$$\mathcal{S}^{1/2} = e^{i\delta_{3/2}} \begin{pmatrix} 1 & 0 & 0 \\ 0 & \frac{1}{3}(1 + 2e^{i\delta}) & -\frac{\sqrt{2}}{3}(1 - e^{i\delta}) \\ 0 & -\frac{\sqrt{2}}{3}(1 - e^{i\delta}) & \frac{1}{3}(2 + e^{i\delta}) \end{pmatrix}, \quad (20)$$

with overall phase $e^{i\delta_{3/2}}$ (i.e. of $A_{D^0\pi^-}$) factored out, and δ is the phase difference between isospin 1/2 and 3/2 amplitudes, which is physical.

An alternative way to obtain $\mathcal{S}^{1/2}$ is through the optical theorem, i.e. Eqs. (5) and (6). This approach is less

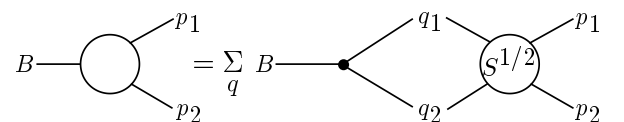


FIG. 3: Illustration of Eq. (16): two body rescattering.

familiar and more awkward than the previous one. However, it has the advantage of being readily generalizable to encompass other modes such as $\bar{B}^0 \rightarrow D^0\eta, D_s^+K^-$, which are now of interest and also provide physical interpretation. To use the optical theorem, we need to study the strong S matrix, or equivalently the T matrix. The T -operator corresponding to the matrix element $M(p_1p_2 \rightarrow q_1q_2)$ for $D\pi \rightarrow D\pi$ scattering in Eqs. (5) and (6) can be written as

$$T = \prod_{i,j=1,2} \int \frac{d^3 p_i}{(2\pi)^3 2E_i} \frac{d^3 q_j}{(2\pi)^3 2E_j} \times (2\pi)^4 \delta^4(p_1 + p_2 - q_1 - q_2) \mathcal{D}^\dagger \mathcal{M} \mathcal{D}', \quad (21)$$

where

$$\begin{aligned} \mathcal{D}^\dagger &= (a_{D^0}(p_1) \ a_{D^+}(p_1)), \quad \mathcal{D}^{\dagger T} = (a_{D^0}^\dagger(q_1) \ a_{D^+}^\dagger(q_1)), \\ \mathcal{M} &= M_0(q_1q_2; p_1p_2) \text{Tr}(\bar{\Pi} \Pi) \mathbf{1} \\ &\quad + M_a(q_1q_2; p_1p_2) \Pi \bar{\Pi} + M_e(q_1q_2; p_1p_2) \bar{\Pi} \Pi, \\ \Pi &= \begin{pmatrix} \frac{1}{\sqrt{2}}a_{\pi^0}(p_2) & a_{\pi^+}(p_2) \\ a_{\pi^-}(p_2) & -\frac{1}{\sqrt{2}}a_{\pi^0}(p_2) \end{pmatrix}, \\ \bar{\Pi} &= \begin{pmatrix} \frac{1}{\sqrt{2}}a_{\pi^0}^\dagger(q_2) & a_{\pi^-}^\dagger(q_2) \\ a_{\pi^+}^\dagger(q_2) & -\frac{1}{\sqrt{2}}a_{\pi^0}^\dagger(q_2) \end{pmatrix}, \end{aligned} \quad (22)$$

and a_M, a_M^\dagger are annihilation and creation operators for the meson M , respectively. Eq. (21) is the most general isospin invariant operator for $D(p_1)\pi(p_2) \rightarrow D'(q_1)\pi'(q_2)$ scattering. The T -operator is defined such that the familiar relation of T matrix (used in Eq. (5)) and amplitude M (used in Eq. (6)) can be reproduced:

$$\langle q_1q_2 | T | p_1p_2 \rangle = (2\pi)^4 \delta^4(q_1 + q_2 - p_1 - p_2) \times M(q_1q_2; p_1p_2). \quad (23)$$

Eq. (21) is unfamiliar as it is expressed directly in creation and annihilation operators. It becomes more familiar when expressed in fields, where we separate out creation and annihilation parts. For example, Π and $\bar{\Pi}$ correspond to the annihilation and creation parts of

$$\begin{pmatrix} \frac{1}{\sqrt{2}}\pi^0 & \pi^+ \\ \pi^- & -\frac{1}{\sqrt{2}}\pi^0 \end{pmatrix},$$

respectively. The SU(2) transformations of Π and $\bar{\Pi}$ can be recognized, since they do not mix creation and annihilation parts. One can find examples of using creation and annihilation operators on the studies of $\pi\pi$, π -nucleon scattering in, for example, Ref. [13].

It is important to note that the $D(p_1)\pi(p_2) \rightarrow D'(q_1)\pi'(q_2)$ scattering amplitudes $M(D\pi \rightarrow D'\pi')$ can be decomposed into the independent amplitudes $M_{0,a,e}(q_1q_2; p_1p_2)$. For example, by using Eqs. (21) and

(22), we have

$$\begin{aligned} M(D^0\pi^- \rightarrow D^0\pi^-) &= M_0 + M_e, \\ M(D^+\pi^- \rightarrow D^+\pi^-) &= M_0 + M_a, \\ M(D^+\pi^- \rightarrow D^0\pi^0) &= \frac{1}{\sqrt{2}}[M_a - M_e] \\ &= M(D^0\pi^0 \rightarrow D^+\pi^-), \\ M(D^0\pi^0 \rightarrow D^0\pi^0) &= M_0 + \frac{1}{2}[M_a + M_e], \end{aligned} \quad (24)$$

where M_i stand for $M_i(q_1q_2; p_1p_2)$. We can now make use of Eq. (6) to obtain $\text{Im } M$. For example,

$$\begin{aligned} 2 \text{Im } A_{D^0\pi^-} &= 2 \text{Im } M(B^- \rightarrow D^0\pi^-) \\ &= \int \frac{d^3 q_1}{(2\pi)^3 2E_1} \frac{d^3 q_2}{(2\pi)^3 2E_2} (2\pi)^4 \delta^4(p_1 + p_2 - q_1 - q_2) \\ &\quad \times M^*(D^0\pi^- \rightarrow D^0\pi^-) A_{D^0\pi^-} \\ &= \int \frac{d^3 q_1}{(2\pi)^3 2E_1} \frac{d^3 q_2}{(2\pi)^3 2E_2} (2\pi)^4 \delta^4(p_1 + p_2 - q_1 - q_2) \\ &\quad \times [M_0^*(q_1q_2; p_1p_2) + M_e^*(q_1q_2; p_1p_2)] A_{D^0\pi^-} \\ &= (r_0^* + r_e^*) A_{D^0\pi^-}, \end{aligned} \quad (25)$$

where

$$\begin{aligned} r_i^* &\equiv \int \frac{d^3 q_1}{(2\pi)^3 2E_1} \frac{d^3 q_2}{(2\pi)^3 2E_2} \\ &\quad \times (2\pi)^4 \delta^4(p_1 + p_2 - q_1 - q_2) M_i^*(q_1q_2; p_1p_2), \end{aligned} \quad (26)$$

for $i = 0, a, e$ and $p_1 + p_2 = p_B$.

Since the $D\pi$ system from B decay is S-wave, $A_{D\pi}$ is independent of the final state momentum. It can hence be factored out from the integration. Thus, Eq. (26) projects out the S-wave $D\pi$ rescattering amplitude. Similar expressions can be obtained for $\text{Im } A_{D^+\pi^-, D^0\pi^0}$. By comparing with Eqs. (5) and (6), we find

$$2 \begin{pmatrix} \text{Im } A_{D^0\pi^-} \\ \text{Im } A_{D^+\pi^-} \\ \text{Im } A_{D^0\pi^0} \end{pmatrix} = \mathcal{T}^\dagger \begin{pmatrix} A_{D^0\pi^-} \\ A_{D^+\pi^-} \\ A_{D^0\pi^0} \end{pmatrix}, \quad (27)$$

$$\mathcal{T}^\dagger = \begin{pmatrix} r_0^* + r_e^* & 0 & 0 \\ 0 & r_0^* + r_a^* & \frac{1}{\sqrt{2}}(r_a^* - r_e^*) \\ 0 & \frac{1}{\sqrt{2}}(r_a^* - r_e^*) & r_0^* + \frac{1}{2}(r_a^* + r_e^*) \end{pmatrix}, \quad (28)$$

with $\mathcal{S} = \mathbf{1} + i\mathcal{T}$. Eq. (27) is consistent with Eq. (16) through the identity $2 \text{Im } \mathcal{S}^{1/2} = \mathcal{T}^\dagger \mathcal{S}^{1/2}$ for symmetric \mathcal{S} . We also note that \mathcal{T} can be diagonalized by using $\mathcal{T} = U^T \mathcal{T}_{\text{diag}} U$, where U is given in Eq. (18), giving

$$\mathcal{T}_{\text{diag}} = \text{diag}(r_0 + r_e, r_0 + r_e, r_0 + \frac{1}{2}(3r_a - r_e)). \quad (29)$$

The unitary scattering matrix $\mathcal{S} = \mathbf{1} + i\mathcal{T}$ can be solved by identifying the elements in $\mathcal{T}_{\text{diag}}$ with $2 \sin(\text{angle}) \exp(i \text{angle})$'s, where we note that $1 +$

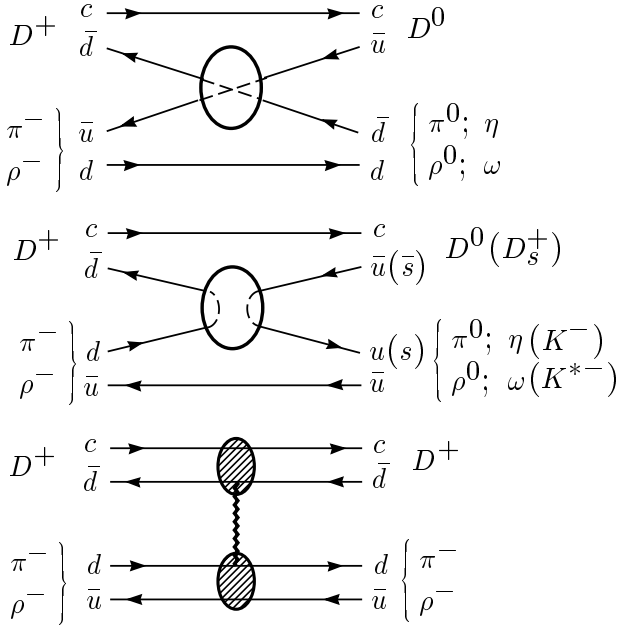


FIG. 4: Pictorial representation of (a) r_e (charge exchange), (b) r_a (annihilation) and (c) r_0 (singlet exchange).

$i 2 \sin(\text{angle}) \exp(i \text{angle}) = \exp(i 2 \text{angle})$. One can now reproduce Eq. (20) by taking

$$\begin{aligned} r_0 + r_e &= 2 \sin \delta_{3/2} e^{i \delta_{3/2}}, \\ r_0 + \frac{1}{2}(3r_a - r_e) &= 2 \sin \delta_{1/2} e^{i \delta_{1/2}}. \end{aligned} \quad (30)$$

We give a pictorial representation of r_e , r_a , r_0 in Fig. 4; they correspond to charge exchange, annihilation, and flavor singlet exchange rescatterings, respectively. Since the quark model is a representation of flavor SU(2) (SU(3)) group, it should be able to reproduce the structure of \mathcal{T} , which follows from symmetry argument. In particular the coefficients of r_i in Eq. (28) can be reproduced easily using this pictorial approach by matching the flavor wave function coefficients. For example, we have $(r_a - r_e)/\sqrt{2}$ for a $D^+ \pi^-$ to $D^0 \pi^0$ rescattering. We see from the first diagram of Fig. 4 that the exchange rescattering (r_e) projects out the $d\bar{d}$ component of π^0 in the right hand side. From our convention in Eq. (8), this give a $-1/\sqrt{2}$ factor from the wave function of π^0 . Similarly the second diagram of Fig. 4 projects out the $u\bar{u}$ component of π^0 and give $r_a/\sqrt{2}$ consequently. These diagrams also provide further information. For example in the second diagram as we go beyond SU(2), it is easy to see that the annihilation rescattering (r_a) is responsible for the $D^+ \pi^- \rightarrow D_s^+ K^-$ rescattering, since there is no s quark before rescattering.

IV. EXTENSION FROM SU(2) TO SU(3)

A. DP Modes

We now generalize the $B \rightarrow D\pi$ case to SU(3) related modes in the final state, such as $\bar{B}^0 \rightarrow D^0 \eta$ or $D_s^+ K^-$. We stress that we apply SU(3) symmetry only towards final state rescattering rather than to the whole decay process. It is thus different from the usual application of SU(3) in B decays [14], where one decomposes the B meson weak decay amplitudes, including the effective Hamiltonian itself, into different SU(3) pieces, and try to relate different modes (oftentimes including B_s decay). As argued earlier, SU(3) should be a good symmetry for energetic FSI rescattering, which is the case of interest. As we will see this approach give identical results with the SU(3) decomposition approach shown in Appendix A.

It is straightforward to follow the steps through Eqs. (21)–(30). Eq. (21) remains unchanged, i.e.

$$T = \prod_{i,j=1,2} \int \frac{d^3 p_i}{(2\pi)^3 2E_i} \frac{d^3 q_j}{(2\pi)^3 2E_j} \times (2\pi)^4 \delta^4(p_1 + p_2 - q_1 - q_2) \mathcal{D}^\dagger \mathcal{M} \mathcal{D}', \quad (31)$$

but now the multiplets are extended

$$\begin{aligned} \mathcal{D}^\dagger &= (a_{D^0}(p_1) \ a_{D^+}(p_1) \ a_{D_s^+}(p_1)), \\ \mathcal{D}'^\text{T} &= (a_{D^0}^\dagger(q_1) \ a_{D^+}^\dagger(q_1) \ a_{D_s^+}^\dagger(q_1)), \\ \mathcal{M} &= M_0(q_1 q_2; p_1 p_2) \text{Tr}(\bar{\Pi} \Pi) \mathbf{1} \\ &\quad + M_a(q_1 q_2; p_1 p_2) \Pi \bar{\Pi} + M_e(q_1 q_2; p_1 p_2) \bar{\Pi} \Pi, \\ \Pi(p_2) &= \begin{pmatrix} \frac{a_{\pi^0}}{\sqrt{2}} + \frac{a_{\eta_8}}{\sqrt{6}} & a_{\pi^+} & a_{K^+} \\ a_{\pi^-} & -\frac{a_{\pi^0}}{\sqrt{2}} + \frac{a_{\eta_8}}{\sqrt{6}} & a_{K^0} \\ a_{K^-} & a_{\bar{K}^0} & -\sqrt{\frac{2}{3}} a_{\eta_8} \end{pmatrix} (p_2), \\ \bar{\Pi}(q_2) &= \begin{pmatrix} \frac{a_{\pi^0}^\dagger}{\sqrt{2}} + \frac{a_{\eta_8}^\dagger}{\sqrt{6}} & a_{\pi^-}^\dagger & a_{K^-}^\dagger \\ a_{\pi^+}^\dagger & -\frac{a_{\pi^0}^\dagger}{\sqrt{2}} + \frac{a_{\eta_8}^\dagger}{\sqrt{6}} & a_{\bar{K}^0}^\dagger \\ a_{K^+}^\dagger & a_{K^0}^\dagger & -\sqrt{\frac{2}{3}} a_{\eta_8}^\dagger \end{pmatrix} (q_2). \end{aligned} \quad (32)$$

Note that this operator can rescatter $D^+ \pi^-$, $D^0 \pi^0$ into the desired states $D^0 \eta_8$, $D_s^+ K^-$.

The physical η , η' mesons are defined through

$$\begin{pmatrix} \eta \\ \eta' \end{pmatrix} = \begin{pmatrix} \cos \vartheta & -\sin \vartheta \\ \sin \vartheta & \cos \vartheta \end{pmatrix} \begin{pmatrix} \eta_8 \\ \eta_1 \end{pmatrix}, \quad (33)$$

where the mixing angle $\vartheta = -15.4^\circ$ [15]. In principle, we should also include $D^0 \eta_1$ in the rescattering process. The additional terms can be obtained by replacing Π in Eq. (32) by $\Pi + \mathbf{1} a_{\eta_1}(q_2)/\sqrt{3}$ (and similarly for $\bar{\Pi}$), and labeling the η_1 related matrix elements by $M'_i(q_1 q_2; p_1 p_2)$.

Knowing that the $U_A(1)$ symmetry is broken by anomaly and η_1 is not a Goldstone boson, M'_i are not identical to M_i . The number of parameters would therefore double, but experimental measurements are still scarce. On the other hand, we note that the mixing angle ϑ is quite small, so we approximate η by η_8 . Thus, we concentrate on the rescattering process involving octet pseudoscalar mesons only, as a step beyond the elastic FSI discussed in the previous section. In this way, as already shown, one again has just three independent amplitudes.

Besides Eq. (24) we now have

$$\begin{aligned} M(D^+\pi^- \rightarrow D^0\eta_8) &= \frac{1}{\sqrt{6}}(M_a + M_e), \\ M(D^+\pi^- \rightarrow D_s^+K^-) &= M_a, \\ M(D^0\pi^0 \rightarrow D^0\eta_8) &= \frac{1}{2\sqrt{3}}(M_a + M_e), \\ M(D^0\pi^0 \rightarrow D_s^+K^-) &= \frac{1}{\sqrt{2}}M_a, \\ M(D^0\eta_8 \rightarrow D^0\eta_8) &= M_0 + \frac{1}{6}(M_a + M_e), \\ M(D^0\eta_8 \rightarrow D_s^+K^-) &= \frac{1}{\sqrt{6}}(M_a - 2M_e), \\ M(D_s^+K^- \rightarrow D_s^+K^-) &= M_0 + M_a, \end{aligned} \quad (34)$$

where M_i stands for $M_i(q_1q_2; p_1p_2)$. Amplitudes for other related modes can be obtained by noting that $M(ab \rightarrow cd) = M(cd \rightarrow ab)$ in our case.

With Eqs. (24), (34) and similar extensions of Eqs. (25) and (26), we extend Eqs. (27) and (28) to $2\text{Im } A = \mathcal{T}^\dagger A$ in the $D^0\pi^-$, $D^+\pi^-$, $D^0\pi^0$, $D^0\eta_8$ and $D_s^+K^-$ basis with

$$\mathcal{T} = r_0 \mathbf{1} + \begin{pmatrix} r_e & 0 & 0 & 0 & 0 \\ 0 & r_a & \frac{r_a - r_e}{\sqrt{2}} & \frac{r_a + r_e}{\sqrt{6}} & r_a \\ 0 & \frac{r_a - r_e}{\sqrt{2}} & \frac{r_a + r_e}{2} & \frac{r_a + r_e}{2\sqrt{3}} & \frac{r_a}{\sqrt{2}} \\ 0 & \frac{r_a + r_e}{\sqrt{6}} & \frac{r_a + r_e}{2\sqrt{3}} & \frac{r_a + r_e}{6} & \frac{r_a - 2r_e}{\sqrt{6}} \\ 0 & r_a & \frac{r_a}{\sqrt{2}} & \frac{r_a - 2r_e}{\sqrt{6}} & r_a \end{pmatrix}, \quad (35)$$

where \mathcal{T} can also be easily obtained by the pictorial approach, as we explain in the end of the previous section. Note that \mathcal{T} can be diagonalized as

$$\mathcal{T}_{\text{diag}} = r_0 \mathbf{1} + \text{diag} \left(r_e, r_e, r_e, -r_e, \frac{1}{3}(8r_a - r_e) \right). \quad (36)$$

Following similar procedure in the previous section, $\mathcal{S} = 1 + i\mathcal{T}$ is obtained by the (physical) substitution

$$\begin{aligned} (1 + ir_0)e^{-2i\delta_{3/2}} &= \frac{1}{2}(1 + e^{2i\delta'}), \\ ir_e e^{-2i\delta_{3/2}} &= \frac{1}{2}(1 - e^{2i\delta'}), \\ ir_a e^{-2i\delta_{3/2}} &= \frac{1}{8}(-1 - 2e^{2i\delta'} + 3e^{2i\theta}), \end{aligned} \quad (37)$$

where $r_0 + r_e = 2\sin\delta_{3/2}e^{i\delta_{3/2}}$ as in Eq. (30), but $\delta = \delta_{1/2} - \delta_{3/2}$ is now extended to two physical phase differences δ' and θ . Note that D , D_s and π , K , η transform as $\bar{3}$ and 8 under $SU(3)$. As shown in Appendix A, we can identify above phases as

$$\delta_{3/2} = \delta_{\bar{15}}, \quad \delta' = \delta_6 - \delta_{\bar{15}}, \quad \theta = \delta_{\bar{3}} - \delta_{\bar{15}}. \quad (38)$$

By analogy to the previous section, the solution of $2\text{Im } A = \mathcal{T}^\dagger A$ is

$$\begin{pmatrix} A_{D^0\pi^-} \\ A_{D^+\pi^-} \\ A_{D^0\pi^0} \\ A_{D^0\eta_8} \\ A_{D_s^+K^-} \end{pmatrix} = \mathcal{S}^{1/2} \begin{pmatrix} A_{D^0\pi^-}^f \\ A_{D^+\pi^-}^f \\ A_{D^0\pi^0}^f \\ A_{D^0\eta_8}^f \\ A_{D_s^+K^-}^f \end{pmatrix}, \quad (39)$$

where A^f s are factorization amplitudes. The matrix $\mathcal{S}^{1/2}$ can be obtained by reducing phases in \mathcal{S} by half. For later purpose, we give the explicit expression of $\mathcal{S}^{1/2}$ (or equivalently \mathcal{S} with trivial modification of phases),

$$\begin{aligned} \mathcal{S}^{1/2} e^{-i\delta_{3/2}} &= \\ &= \begin{pmatrix} 1 & 0 & 0 & 0 & 0 \\ 0 & \frac{1}{8}(3 + 2e^{i\delta'} + 3e^{i\theta}) & \frac{1}{8\sqrt{2}}(-5 + 2e^{i\delta'} + 3e^{i\theta}) & \frac{1}{8}\sqrt{\frac{3}{2}}(1 - 2e^{i\delta'} + e^{i\theta}) & -\frac{1}{8}(1 + 2e^{i\delta'} - 3e^{i\theta}) \\ 0 & \frac{1}{8\sqrt{2}}(-5 + 2e^{i\delta'} + 3e^{i\theta}) & \frac{1}{16}(11 + 2e^{i\delta'} + 3e^{i\theta}) & \frac{\sqrt{3}}{16}(1 - 2e^{i\delta'} + e^{i\theta}) & -\frac{1}{8\sqrt{2}}(1 + 2e^{i\delta'} - 3e^{i\theta}) \\ 0 & \frac{1}{8}\sqrt{\frac{3}{2}}(1 - 2e^{i\delta'} + e^{i\theta}) & \frac{\sqrt{3}}{16}(1 - 2e^{i\delta'} + e^{i\theta}) & \frac{1}{16}(9 + 6e^{i\delta'} + e^{i\theta}) & \frac{1}{8}\sqrt{\frac{3}{2}}(-3 + 2e^{i\delta'} + e^{i\theta}) \\ 0 & -\frac{1}{8}(1 + 2e^{i\delta'} - 3e^{i\theta}) & -\frac{1}{8\sqrt{2}}(1 + 2e^{i\delta'} - 3e^{i\theta}) & \frac{1}{8}\sqrt{\frac{3}{2}}(-3 + 2e^{i\delta'} + e^{i\theta}) & \frac{1}{8}(3 + 2e^{i\delta'} + 3e^{i\theta}) \end{pmatrix}. \end{aligned} \quad (40)$$

Just as in Eqs. (16) and (20), $\mathcal{S}^{1/2}$ of Eq. (40) has an overall phase. Only phase differences affect decay rates. An overall sign change of the phases also leaves rates unchanged.

Note that charge conservation and unitarity imply,

$$\begin{aligned} |A_{D^0\pi^-}|^2 &= |A_{D^0\pi^-}^f|^2, \\ |A_{D^+\pi^-}|^2 + |A_{D^0\pi^0}|^2 + |A_{D^0\eta_8}|^2 + |A_{D_s^+K^-}|^2 &= |A_{D^+\pi^-}^f|^2 + |A_{D^0\pi^0}^f|^2 + |A_{D^0\eta_8}^f|^2 + |A_{D_s^+K^-}^f|^2. \end{aligned} \quad (41)$$

Since the amplitudes for color suppressed modes are small at the factorization level, they will be fed by the color allowed amplitude $A_{D^+\pi^-}^f$. As a consequence, the $D^+\pi^-$ rate will be reduced from its factorization result. Compared with the elastic case, we now have additional, but slight, leakage of $D^+\pi^-$ into $D^0\eta$ and $D_s^+K^-$ modes. Because the measured rates of color suppressed modes are still small as compared to the color allowed modes, as far as the $D\pi$ system is concerned, the results do not deviate too much from the previous section.

On the other hand, since the factorization amplitudes $A_{D\pi}^f$ satisfy the isospin triangular relation, Eq. (13), one can show that, with FSI and for any value of $A_{D^0\eta_8}^f$ and $A_{D_s^+K^-}^f$, the rescattered $A_{D\pi}$ amplitudes also satisfy the relation. As noted earlier, the isospin relation should hold whether FSI is active or not. To demonstrate this, it is instructive to express the FSI of Eq. (40) in the isospin basis. In the $D^0\pi^-$, $(D\pi)_{3/2}$, $(D\pi)_{1/2}$, $D^0\eta_8$ and $D_s^+K^-$ basis, the \mathcal{T} matrix, and similarly $\mathcal{S}^{(1/2)}$, take a block diagonal form

$$\mathcal{T}_{\text{block}} = r_0 \mathbf{1} + \begin{pmatrix} r_e & 0 & 0 & 0 & 0 \\ 0 & r_e & 0 & 0 & 0 \\ 0 & 0 & \frac{3r_a - r_e}{2} & \frac{r_a + r_e}{2} & \sqrt{\frac{3}{2}}r_a \\ 0 & 0 & \frac{r_a + r_e}{2} & \frac{r_a + r_e}{6} & \frac{r_a - 2r_e}{\sqrt{6}} \\ 0 & 0 & \sqrt{\frac{3}{2}}r_a & \frac{r_a - 2r_e}{\sqrt{6}} & r_a \end{pmatrix}, \quad (42)$$

by $\mathcal{T}_{\text{block}} = O \mathcal{T} O^T$, where

$$O = \begin{pmatrix} U & 0 & 0 \\ 0 & 1 & 0 \\ 0 & 0 & 1 \end{pmatrix}, \quad (43)$$

and U is given in Eq. (18). Truncating to the first 3×3 sub-matrix, \mathcal{T} is diagonal and one reproduces the SU(2) case of Eq. (29).

In this basis, with block diagonalized $\mathcal{S}_{\text{block}}^{1/2} = O \mathcal{S}^{1/2} O^T$, Eq. (39) becomes

$$A = \mathcal{S}_{\text{block}}^{1/2} A^f, \quad (44)$$

where the first two diagonal elements of $\mathcal{S}_{\text{block}}^{1/2}$ are just $e^{i\delta_{3/2}}$, while the remaining lower block governs the “in-

elastic” rescatterings

$$\begin{aligned} e^{-i\delta_{3/2}} (\mathcal{S}_{\text{block}}^{1/2})_{(D\pi)_{1/2}, (D\pi)_{1/2}} &= \frac{1}{16}(1 + 6e^{i\delta'} + 9e^{i\theta}), \\ e^{-i\delta_{3/2}} (\mathcal{S}_{\text{block}}^{1/2})_{(D\pi)_{1/2}, D^0\eta_8} &= \frac{3}{16}(1 - 2e^{i\delta'} + e^{i\theta}), \\ e^{-i\delta_{3/2}} (\mathcal{S}_{\text{block}}^{1/2})_{(D\pi)_{1/2}, D_s^+K^-} &= -\frac{\sqrt{3}}{8\sqrt{2}}(1 + 2e^{i\delta'} - 3e^{i\theta}), \\ e^{-i\delta_{3/2}} (\mathcal{S}_{\text{block}}^{1/2})_{D^0\eta_8, D^0\eta_8} &= \frac{1}{16}(9 + 6e^{i\delta'} + e^{i\theta}), \\ e^{-i\delta_{3/2}} (\mathcal{S}_{\text{block}}^{1/2})_{D^0\eta_8, D_s^+K^-} &= \frac{\sqrt{3}}{8\sqrt{2}}(-3 + 2e^{i\delta'} + e^{i\theta}), \\ e^{-i\delta_{3/2}} (\mathcal{S}_{\text{block}}^{1/2})_{D_s^+K^-, D_s^+K^-} &= \frac{1}{8}(3 + 2e^{i\delta'} + 3e^{i\theta}). \end{aligned} \quad (45)$$

between the $I = I_z = 1/2$ decay final states $(D\pi)_{1/2}$, $D^0\eta_8$ and $D_s^+K^-$, which is a reasonable extension beyond the elastic rescattering discussed in the previous section. The elastic case corresponds to $e^{-i\delta_{3/2}} (\mathcal{S}_{\text{block}}^{1/2})_{(D\pi)_{1/2}, (D\pi)_{1/2}} = e^{i\delta}$ and setting the rest of Eq. (45) to zero. Since the factorization amplitudes for $D^0\eta$ and $D_s^+K^-$ are small, their FSI contribution to the $D\pi$ system will be suppressed. Therefore,

$$\begin{aligned} \left| \frac{A_{1/2}}{A_{1/2}^f} \right| &\sim \left| \frac{1}{16}(1 + 6e^{i\delta'} + 9e^{i\theta}) \right|, \\ \delta &\sim \arg(1 + 6e^{i\delta'} + 9e^{i\theta}), \end{aligned} \quad (46)$$

are good estimates. The geometric meaning of Eq. (45) is given in Appendix B.

B. D^*P and DV Modes

The formalism can be applied to final states involving pseudoscalar and vector mesons (PV), with only slight modifications.

For $D^*(p_1; \lambda)P(p_2) \rightarrow D^*(q_1; \lambda')P'(q_2)$ rescattering, where $\lambda^{(i)}$ is the polarization index and $P^{(i)}$ denotes a pseudoscalar meson, we replace $a_D(p_1)$ and $M_i(q_1 q_2; p_1 p_2)$ by $a_{D^*}(p_1, \lambda)$ and $M_i(q_1 q_2, \lambda'; p_1 p_2, \lambda)$ etc., respectively, where

$$\begin{aligned} \langle q_1 q_2, \lambda' | T | p_1 p_2, \lambda \rangle \\ = (2\pi)^4 \delta^4(p_1 + p_2 - q_1 - q_2) M(q_1 q_2, \lambda'; p_1 p_2, \lambda). \end{aligned} \quad (47)$$

The $B \rightarrow D^*P$ amplitude is expressed as

$$M(B \rightarrow D^*P) = \varepsilon_\lambda^* \cdot p_B A_{D^*P}, \quad (48)$$

where ε_λ is the polarization vector and A_{D^*P} is a Lorentz scalar that is independent of ε and the angle between the 3-momenta of D^* and P .

Take $B^- \rightarrow D^{*0}\pi^-$ for example. Eq. (25) becomes

$$\begin{aligned} & 2 \operatorname{Im} [(\varepsilon_\lambda^* \cdot p_B) A_{D^{*0}\pi^-}] \\ &= \sum_{\lambda'} \int \frac{d^3 q_1}{(2\pi)^3 2E_1} \frac{d^3 q_2}{(2\pi)^3 2E_2} (2\pi)^4 \delta^4(p_1 + p_2 - q_1 - q_2) \\ & \quad \times [M_0^*(q_1 q_2, \lambda'; p_1 p_2, \lambda) + M_e^*(q_1 q_2, \lambda'; p_1 p_2, \lambda)] \\ & \quad \times \varepsilon_{\lambda'}^* \cdot p_B A_{D^{*0}\pi^-}. \end{aligned} \quad (49)$$

By choosing a real basis for ε and noting that $\sum_\lambda (p_B \cdot \varepsilon_\lambda)^2 = p_{cm}^2 m_B^2 / m_{D^{*0}}^2$, where p_{cm} is the momentum of D^{*0} in the center of mass frame, we obtain

$$2 \operatorname{Im} A_{D^{*0}\pi^-} = (r_0^* + r_e^*) A_{D^{*0}\pi^-}, \quad (50)$$

with

$$\begin{aligned} r_i^* \equiv & \sum_{\lambda\lambda'} \int \frac{d^3 q_1}{(2\pi)^3 2E_1} \frac{d^3 q_2}{(2\pi)^3 2E_2} \\ & \times (2\pi)^4 \delta^4(p_1 + p_2 - q_1 - q_2) \frac{m_{D^{*0}}^2}{m_B^2 p_{cm}^2} \\ & \times \varepsilon_\lambda \cdot p_B M_i^*(q_1 q_2 \lambda'; p_1 p_2, \lambda) \varepsilon_{\lambda'} \cdot p_B, \end{aligned} \quad (51)$$

which projects out the P-wave D^*P scattering amplitude. Equations after Eq. (32) from previous section can be carried over by replacing $A_{DP} \rightarrow A_{D^*P}$.

The generalization to DV decay modes is again straightforward, except that ω_1 – ω_8 mixing cannot be neglected. The physical mesons should be

$$\begin{aligned} \omega &= \sqrt{\frac{2}{3}}\omega_1 + \sqrt{\frac{1}{3}}\omega_8, \\ \phi &= \sqrt{\frac{1}{3}}\omega_1 - \sqrt{\frac{2}{3}}\omega_8. \end{aligned} \quad (52)$$

Unlike the pseudoscalar case, where ignoring η_1 couplings can be partially justified, ω_1 in principle should be on similar footing as ω_8 .

We replace π , K and η_8 in Eq. (32) by ρ , K^* and ω_8 . By including ω_1 we will have two more terms in \mathcal{M} of the corresponding T matrix namely, $a_{\omega_1}^\dagger(q_2) a_{\omega_1}(p_2) [\widetilde{M}_0 + (\widetilde{M}_a + \widetilde{M}_e)/3]$ and $[a_{\omega_1}(p_2) \bar{\Pi} + \Pi a_{\omega_1}^\dagger(q_2)] (\overline{M}_a + \overline{M}_e)/\sqrt{3}$. These two terms correspond to ω_1 to ω_1 and ω_1 to octet rescattering. These \widetilde{M}_i , \overline{M}_i will reduce to M_i under nonet symmetry.

The \mathcal{T} matrix can be obtained as before. In isospin basis with the $D^0\rho^-$, $(D\rho)_{3/2}$, $(D\rho)_{1/2}$, $D^0\omega_8$, $D_s^+K^{*-}$ and $D^0\omega_1$, we have

$$\begin{aligned} \mathcal{T}_{\text{block}} &= \operatorname{diag}(r_0, r_0, r_0, r_0, r_0, \tilde{r}_0) \\ &+ \begin{pmatrix} r_e & 0 & 0 & 0 & 0 & 0 \\ 0 & r_e & 0 & 0 & 0 & 0 \\ 0 & 0 & \frac{3r_a - r_e}{2} & \frac{r_a + r_e}{2} & \sqrt{\frac{3}{2}}r_a & \frac{\bar{r}_a + \bar{r}_e}{\sqrt{2}} \\ 0 & 0 & \frac{r_a + r_e}{2} & \frac{r_a + r_e}{6} & \frac{r_a - 2r_e}{\sqrt{6}} & \frac{\bar{r}_a + \bar{r}_e}{3\sqrt{2}} \\ 0 & 0 & \sqrt{\frac{3}{2}}r_a & \frac{r_a - 2r_e}{\sqrt{6}} & r_a & \frac{\bar{r}_a + \bar{r}_e}{\sqrt{3}} \\ 0 & 0 & \frac{\bar{r}_a + \bar{r}_e}{\sqrt{2}} & \frac{\bar{r}_a + \bar{r}_e}{3\sqrt{2}} & \frac{\bar{r}_a + \bar{r}_e}{\sqrt{3}} & \frac{\tilde{r}_a + \tilde{r}_e}{3} \end{pmatrix}. \end{aligned} \quad (53)$$

It can also be easily obtained by the pictorial approach in the ω_1 , ω_8 basis. $\mathcal{T}_{\text{block}}$ is identical to Eq. (42) except the additional sixth row and column. The solution is, $r_{0,e}$ as shown in Eq. (37) and

$$\begin{aligned} ir_a e^{-2i\delta_{3/2}} &= \frac{1}{8}(3\mathcal{U}_{\overline{3}\overline{3}} e^{-2i\delta_{3/2}} - 2e^{2i\delta'} - 1), \\ i(\bar{r}_a + \bar{r}_e) &= \frac{3}{2\sqrt{2}}\mathcal{U}_{\overline{3}\overline{3}'}, \\ i(\tilde{r}_0 + \frac{\tilde{r}_a + \tilde{r}_e}{3}) &= \mathcal{U}_{\overline{3}'\overline{3}'} - 1, \end{aligned} \quad (54)$$

where \mathcal{U} is a two by two symmetric unitary matrix that mixes $\overline{\mathbf{3}}$ and $\overline{\mathbf{3}'}$ by rescattering as shown in Appendix A. Note that we need two phases and one mixing angle to specify \mathcal{U} , resulting four parameters (with an overall phase factored out) to describe the rescattering matrix. There are too many parameters and experiment measurements are still scarce. However, there is no $U_A(1)$ anomaly in the vector sector, and we expect $U(3)$ rather than $SU(3)$ symmetry. Therefore we consider rescattering among $D^{0,+}$, D_s^+ and the vector nonet as a first step beyond the simple elastic FSI case. In this case we identify \bar{r}_i and \tilde{r}_i as r_i .

It turns out that $U(3)$ symmetry allows only either charge exchange or annihilation FSI, but not both. The two distinct solutions for r_i and \mathcal{U} are

Solution 1:

$$\begin{aligned} (1 + ir_0) e^{-2i\delta_{3/2}} &= \frac{1}{2}(1 + e^{2i\delta'}), \\ ir_e e^{-2i\delta_{3/2}} &= \frac{1}{2}(1 - e^{2i\delta'}), \\ ir_a e^{-2i\delta_{3/2}} &= 0, \\ \mathcal{U}_{\overline{3}\overline{3}} e^{-2i\delta_{3/2}} &= \frac{1}{3}(1 + 2e^{2i\delta'}), \\ \mathcal{U}_{\overline{3}\overline{3}'} e^{-2i\delta_{3/2}} &= \frac{\sqrt{2}}{3}(1 - e^{2i\delta'}), \\ \mathcal{U}_{\overline{3}'\overline{3}'} e^{-2i\delta_{3/2}} &= \frac{1}{3}(2 + e^{2i\delta'}), \end{aligned} \quad (55)$$

Solution 2:

$$\begin{aligned} (1 + ir_0^{(\prime)}) e^{-(2)i\delta_{3/2}} &= 1, \\ ir_e^{(\prime)} e^{-(2)i\delta_{3/2}} &= 0, \\ ir_a^{(\prime)} e^{-(2)i\delta_{3/2}} &= \frac{1}{3}(-1 + e^{(2)i\sigma}), \\ \mathcal{U}_{\overline{3}\overline{3}} e^{-2i\delta_{3/2}} &= \frac{1}{9}(1 + 8e^{2i\sigma}), \\ \mathcal{U}_{\overline{3}\overline{3}'} e^{-2i\delta_{3/2}} &= \frac{2\sqrt{2}}{9}(-1 + e^{2i\sigma}), \\ \mathcal{U}_{\overline{3}'\overline{3}'} e^{-2i\delta_{3/2}} &= \frac{1}{9}(8 + e^{2i\sigma}), \end{aligned} \quad (56)$$

where the former (latter) does not have annihilation (exchange) contribution. Notice that while $\delta' \equiv \delta_6 - \delta_{\overline{15}}$ is analogous to the $D^{(*)}P$ counterpart, σ is from \mathcal{U} and is not equivalent to θ .

To understand why $r_a r_e = 0$, we show the \mathcal{T} matrix in the $D^0 \rho^-$, $D^+ \rho^-$, $D^0 \rho^0$, $D^0 \omega$, $D_s^+ K^{*-}$ and $D^0 \phi$ basis.

$$\mathcal{T}_V = r_0 \mathbf{1} + \begin{pmatrix} r_e & 0 & 0 & 0 & 0 & 0 \\ 0 & r_a & \frac{r_a - r_e}{\sqrt{2}} & \frac{r_a + r_e}{\sqrt{2}} & r_a & 0 \\ 0 & \frac{r_a - r_e}{\sqrt{2}} & \frac{r_a + r_e}{2} & \frac{r_a + r_e}{2} & \frac{r_a}{\sqrt{2}} & 0 \\ 0 & \frac{r_a + r_e}{\sqrt{2}} & \frac{r_a + r_e}{2} & \frac{r_a + r_e}{2} & \frac{r_a}{\sqrt{2}} & 0 \\ 0 & r_a & \frac{r_a}{\sqrt{2}} & \frac{r_a}{\sqrt{2}} & r_a & r_e \\ 0 & 0 & 0 & 0 & r_e & 0 \end{pmatrix}. \quad (57)$$

Note that $\mathcal{T}_V^{6i} = 0$ for $i = 2, 3, 4$, so $D^0 \phi$ can only rescatter with itself and $D_s^+ K^{*-}$. This can be easily checked by using the pictorial method as shown in Fig. 4.

We define \mathcal{T}'_V via $\mathcal{S}_V^{1/2} = 1 + i\mathcal{T}'_V$. It is easy to show that $\mathcal{T}_V = 2\mathcal{T}'_V + i\mathcal{T}^2_V$. $\mathcal{S}_V^{1/2}$ should also satisfy the U(3) symmetry as well since it is generated by the same dynamics (or Hamiltonian) as \mathcal{S}_V . Since the construction of \mathcal{T}_V is based on symmetry, we expect \mathcal{T}'_V to have the same structure, or simply with $r_{0,a,e}$ replaced by $r'_{0,a,e}$. It is then easy to show that

$$\mathcal{T}_V^{6j} = i(\mathcal{T}'_V)^{6j} \propto r'_a r'_e, \quad (58)$$

for $j = 2, 3, 4$. Since these elements of \mathcal{T}_V are zero, we must have $r'_a r'_e = 0$ which implies $r_a r_e = 0$.

With these r'_i , which are r_i in Eqs. (55), (56) with phases reduced by half, we obtain the decay amplitudes by applying $A = \mathcal{S}_V^{1/2} A^f$.

V. NUMERICAL ANALYSIS

A. $\overline{B} \rightarrow DP$ and D^*P Modes

For $\overline{B} \rightarrow D\pi$ modes, we start from Eq. (14), where the factorization amplitudes are decomposed into color-allowed external W -emission (T), color-suppressed internal W -emission (C), and W -exchange amplitude (E). They are given by [4, 16]

$$\begin{aligned} T &= \frac{G_F}{\sqrt{2}} V_{cb} V_{ud}^* a_1 (m_B^2 - m_D^2) f_\pi F_0^{BD}(m_\pi^2), \\ C &= \frac{G_F}{\sqrt{2}} V_{cb} V_{ud}^* a_2 (m_B^2 - m_\pi^2) f_D F_0^{B\pi}(m_D^2), \\ E &= \frac{G_F}{\sqrt{2}} V_{cb} V_{ud}^* a_2 (m_D^2 - m_\pi^2) f_B F_0^{0 \rightarrow D\pi}(m_B^2). \end{aligned} \quad (59)$$

Since the annihilation form factor $F_0^{0 \rightarrow D\pi}(m_B^2)$ is expected to be suppressed at $q^2 = m_B^2$ and a_2 is small, the amplitude E is neglected. For $\overline{B}^0 \rightarrow D^0 \eta$ we have

$$A_{D^0 \eta}^f = \frac{G_F}{\sqrt{2}} V_{cb} V_{ud}^* a_2 (m_B^2 - m_\eta^2) f_D F_0^{B\eta}(m_D^2), \quad (60)$$

where $\eta_1 - \eta_8$ mixing effect is included via $F_0^{B\eta}(m_D^2) = \cos \vartheta F_0^{B\eta_8} - \sin \vartheta F_0^{B\eta_1}$. We use experimentally measured

TABLE I: Form factors in LF and NS form-factor models where $A_i^{B\omega}(q^2) = A_i^{B\rho}(q^2)/\sqrt{2}$ and $V^{B\omega}(q^2) = V^{B\rho}(q^2)/\sqrt{2}$.

	LF (NS)	LF (NS)	
$F_0^{B\pi}(m_D^2)$	0.29 (0.27)	$A_0^{BD^*}(m_\pi^2)$	0.73 (0.64)
$F_1^{B\pi}(m_{D^*}^2)$	0.34 (0.32)	$A_0^{B\rho}(m_D^2)$	0.35 (0.31)
$F_0^{B\eta}(m_D^2)$	0.16 (0.15)	$A_1^{B\rho}(m_{D^*}^2)$	0.23 (0.28)
$F_1^{B\eta}(m_{D^*}^2)$	0.19 (0.18)	$A_2^{B\rho}(m_{D^*}^2)$	0.22 (0.31)
$F_0^{BD}(m_\pi^2)$	0.70 (0.63)	$V^{B\rho}(m_{D^*}^2)$	0.30 (0.32)
$F_0^{BD}(m_K^2)$	0.70 (0.64)	$A_0^{BD^*}(m_K^2)$	0.74 (0.65)
$F_0^{BD}(m_{K^*}^2)$	0.71 (0.65)	$A_0^{BK^*}(m_D^2)$	0.40 (0.35)
$F_0^{BK}(m_D^2)$	0.42 (0.31)	$F_1^{BK}(m_{D^*}^2)$	0.44 (0.36)

masses in $A_{D^0\pi^-}^f$, $A_{D^+\pi^-}^f$, $A_{D^0\pi^0}^f$ and $A_{D^0\eta}^f$. These amplitudes are real in our phase convention.

For $\overline{B} \rightarrow D^* \pi$, $D^{*0} \eta$, we have $M(\overline{B} \rightarrow D^* P) = (\varepsilon \cdot p_B) A_{D^* P}$ [Eq. (48)]. Analogous to Eq. (14), the factorization amplitudes $A_{D^* \pi}^f$ are decomposed into

$$\begin{aligned} T &= \frac{G_F}{\sqrt{2}} V_{cb} V_{ud}^* a_1 f_\pi 2m_{D^*} A_0^{BD}(m_\pi^2), \\ C &= \frac{G_F}{\sqrt{2}} V_{cb} V_{ud}^* a_2 f_{D^*} 2m_{D^*} F_1^{B\pi}(m_D^2), \end{aligned} \quad (61)$$

where E is again neglected. For $\overline{B}^0 \rightarrow D^{*0} \eta$ we have

$$A_{D^{*0} \eta}^f = \frac{G_F}{\sqrt{2}} V_{cb} V_{ud}^* a_2 f_{D^*} 2m_{D^*} F_1^{B\eta}(m_D^2). \quad (62)$$

Starting from $A_{D^{(*)}P}^f$, FSI redistributes these sources into the amplitudes $\tilde{A}_{D^{(*)}P}$, and we obtain the corresponding rates by,

$$\begin{aligned} \Gamma(\overline{B} \rightarrow PP) &= |A_{PP}|^2 p_{\text{cm}} / (8\pi m_B^2), \\ \Gamma(\overline{B} \rightarrow VP) &= |A_{VP}|^2 p_{\text{cm}}^3 / (8\pi m_V^2), \end{aligned} \quad (63)$$

where

$$2m_B p_{\text{cm}} = \sqrt{[m_B^2 - (m_1 + m_2)^2][m_B^2 - (m_1 - m_2)^2]}. \quad (64)$$

Note that we factor out $\varepsilon \cdot p_B$ in the definition of the amplitude A_{VP} , so our expression for $\Gamma(B \rightarrow VP)$ is slightly different from that in Ref. [16].

In our numerical study, we fix $V_{ud} = 0.9749$, $V_{us} = 0.2225$, $V_{cb} = 0.04$, and use the decay constants $f_\pi = 133$ MeV, $f_{K^{(*)}} = 158$ (214) MeV, $f_{D^{(*)}} = 200$ (230) MeV and $f_\rho = 210$ MeV. Masses and lifetimes are taken from Particle Data Group (PDG) [3]. We consider two form factor models: the relativistic light-front (LF) quark model [17] and Neubert-Stech (NS) model [4]. The relevant values are listed in Table I. We use the color suppressed branching ratios of Belle [1], except for $D^{(*)0} \pi^0$ modes where we combine with the latest CLEO numbers [2]. For other modes we use PDG values [3]. Since the charged $D^{(*)0} \pi^-$ mode does not rescatter to other modes, we normalize all modes to $\mathcal{B}(D^{(*)0} \pi^-) = [5.3 (4.6) \pm 0.5 (0.4)] \times 10^{-3}$

TABLE II: The best fits in the SU(3) FSI picture. The subscript indicates DP or D^*P modes. Form factor model dependence is less than a couple of %.

	Fit1 $_{DP}$	Fit2 $_{DP}$	Fit $_{D^*P}$
χ^2	0.20	0.27	0.21
δ'	47.8°	17.1°	55.7°
θ	24.8°	-52.7°	18.2°
$(1 + ir_0)e^{-2i\delta_{3/2}}$	$0.45 + 0.50i$	$0.91 + 0.28i$	$0.32 + 0.47i$
$ir_e e^{-2i\delta_{3/2}}$	$0.55 - 0.50i$	$0.09 - 0.28i$	$0.68 - 0.47i$
$ir_a e^{-2i\delta_{3/2}}$	$0.14 + 0.04i$	$-0.43 - 0.50i$	$0.27 - 0.01i$
$ A_{1/2}/(\sqrt{2}A_{3/2}) $	0.75	0.65	0.71
$ \delta_{1/2} - \delta_{3/2} $	30.2°	26.2°	28.3°

[3]. We then perform a χ^2 fit to the ratios of branching ratios $\mathcal{B}(D^{(*)+}\pi^-)/\mathcal{B}(D^{(*)0}\pi^-)$, $\mathcal{B}(D^{(*)0}\pi^0)/\mathcal{B}(D^{(*)0}\pi^-)$ and $\mathcal{B}(D^{(*)0}\eta)/\mathcal{B}(D^{(*)0}\pi^-)$.

The use of ratios reduces model dependence on form factors, and is sensitive only to a_2/a_1 . Our numerical results for rescattering phases in LF and NS form factor models never differ by more than a few %. With $|a_2| = 0.26 \pm 0.02$ from fit to $B \rightarrow J/\psi K$ data [16] and the range of $a_1 \sim 1\text{--}1.1$, $a_2 \sim 0.2\text{--}0.3$ from various modes [4], we shall adopt $a_2/a_1 = 0.25$ in subsequent discussion. We find that a larger a_2/a_1 is preferred for the DP modes, but the converse is true for D^*P modes. However, for $a_2/a_1 \approx 0.25$, the χ^2 s of best fits to DP and D^*P modes are both quite small.

The best fits for FSI phase differences δ' and θ (or alternatively the rescattering parameters r_i) are given in Table II. We do not list form factor model dependence since it shows up often only at third decimal place. We find two fits for the DP case, but only one fit for the D^*P modes. For DP modes, the set that we call ‘‘Fit1’’ is similar to the D^*P modes, i.e. $\delta' \sim \pm 50^\circ$, $\theta \sim \pm 20^\circ$. We find that the quark exchange strength $|r_e|$ is larger than the annihilation strength $|r_a|$ in this case. As illustrated in Appendix B, the large phase $\sim 50^\circ$ arises because of sizable strength of both $D^{(*)0}\pi^0$ and $D^{(*)0}\eta$. While δ' and θ effects are of similar sign for the former, for the latter they counteract, and a large δ' phase is needed.

For ‘‘Fit2’’ of the DP case, we have $\delta' \sim \pm 20^\circ$, $\theta \sim \mp 50^\circ$, implying that $|r_a| > |r_e|$. As we will see later, this fit is ruled out by the $\bar{B}^0 \rightarrow D_s^+ K^-$ bound. We mention a curious point about our ‘‘Pomeron’’ related effect, i.e. $|1 + ir_0| = 0.67$, 0.95 and 0.57 , respectively, for Fit1 $_{DP}$, Fit2 $_{DP}$ and Fit $_{D^*P}$. The first and the last are remarkably consistent with the estimates of $S_{\pi\pi \rightarrow \pi\pi} \sim 0.58$ [18], 0.68 and $S_{D\pi \rightarrow D\pi} \sim 0.76$ [9] at $\sqrt{s} = m_B$. In contrast, Fit2 $_{DP}$, which is already ruled out by data, is not quite consistent.

In Table II we show $|A_{1/2}/(\sqrt{2}A_{3/2})|$ and $|\delta_{1/2} - \delta_{3/2}|$ obtained by using the fitted strong phases. The comparison with Eq. (15) will be discussed in the next section.

We summarize the predicted rates of various modes in Table III. The branching ratios are obtained by multiplying the fitted ratios of branching ratios by the

TABLE III: The branching ratios of various $D^{(*)}P$ modes in 10^{-4} units. The second and third columns compare experiment with factorization model. The last two columns give the best fit results with FSI parameters of Table II.

Mode	$\mathcal{B} (\times 10^{-4})$	fac ^{LF (NS)}	Fit1 $_{DP}$	Fit $_{D^*P}$
χ^2	–	–	0.20	0.21
$D^+\pi^-$	30 ± 4	$35.7 (35.5)$	32.2	–
$D^0\pi^0$	2.9 ± 0.5	$0.57 (0.58)$	2.93	–
$D^0\eta$	$1.4^{+0.5}_{-0.4} \pm 0.3$	$0.33 (0.34)$	1.43	–
$D_s^+K^-$	$< 2.4 (0.7)$	0	0.03	–
$D^{*+}\pi^-$	27.6 ± 2.1	$29.8 (29.0)$	–	26.3
$D^{*0}\pi^0$	2.5 ± 0.7	$0.60 (0.69)$	–	2.44
$D^{*0}\eta$	$2.0^{+0.9}_{-0.8} \pm 0.4$	$0.34 (0.39)$	–	1.83
$D_s^{*+}K^-$	< 1.7	0	–	0.16

measured central value of $\mathcal{B}(D^{(*)0}\pi^-)$. The results for $D^{(*)+}\pi^-$, $D^{(*)0}\pi^0$, $D^{(*)0}\eta$ fit the data well, as expected from the small χ^2 . It is worthy to note that rates given in Table III satisfy the unitarity condition of Eq. (4), i.e., the sum of branching ratios before and after FSI is equal as shown in Eq. (41), up to small phase space corrections. This clearly shows that the color suppressed modes are fed from the $D^{(*)+}\pi^-$ mode.

At the amplitude level, one reads from Eq. (35) that $D^{(*)0}\pi^0$, $D^{(*)0}\eta$ and $D_s^{(*)+}K^-$ receive the $(r_a - r_e)/\sqrt{2}$, $(r_a + r_e)/\sqrt{6}$ and r_a rescatterings, respectively, from $D^{(*)+}\pi^-$. Indeed, by using phases shown in Table II in Eq. (40), the FSI contribution can be estimated by using $|A_{D^{(*)0}\pi^0}/A_{D^{(*)+}\pi^-}| \sim |\mathcal{S}_{D^{(*)+}\pi^-, D^{(*)0}\pi^0}^{1/2}|$ and similarly for $|A_{D^{(*)0}\eta}|$ and $|A_{D_s^{(*)+}K^-}|$. The FSI contribution from $D^{(*)+}\pi^-$ alone provides 70%–80% of measured $D^{(*)0}\pi^0$, $D^{(*)0}\eta$ rates, with the remainder coming from a_2 and interference terms. For the $D_s^{(*)+}K^-$ mode, the FSI contribution from $D^{(*)+}\pi^-$ is small due to the smallness of r_a but it is still three times larger than that shown in Table III. Because of this smallness, the FSI rescattering from the color suppressed modes (due to the non-vanishing a_2) through r_e cannot be neglected, which reduces the rate to that shown in the Table.

We note that the factorized a_2 contribution to color suppressed modes show some form factor model dependence, especially for D^*P modes, but such model dependence for fit results are rather slight. The reduced form factor dependence is quite consistent with FSI rescattering dominance over factorized a_2 amplitude, since $D^{(*)+}\pi^-$ is the common source.

In ‘‘Fit2’’ we find $\mathcal{B}(D_s^+K^-) = 4.65 \times 10^{-4} > \mathcal{B}(D^0\pi^0)$, $\mathcal{B}(D^0\eta)$ due to $|r_a| > |r_e|$. This value is above the PDG bound of $\mathcal{B}(D_s^+K^-) < 2.4 \times 10^{-4}$, and way above the recent Belle bound of 0.7×10^{-4} [19], hence is ruled out. The results for Fit2 are therefore not shown in Table III. On the other hand, since $|r_a|$ in the D^*P case is not too small, the result of $\mathcal{B}(D_s^{*+}K^-) \sim 1.6 \times 10^{-5}$ may still be of interest.

B. FSI in DV modes

For $\overline{B} \rightarrow D\rho$, $D\omega$, we have $M(\overline{B} \rightarrow DV) = \varepsilon \cdot p_B A_{DV}$ and $A_{D\rho}^f$ can be decomposed into

$$\begin{aligned} T &= \frac{G_F}{\sqrt{2}} V_{cb} V_{ud}^* a_1 f_\rho 2m_\rho F_0^{BD}(m_\rho^2), \\ C &= \frac{G_F}{\sqrt{2}} V_{cb} V_{ud}^* a_2 f_D 2m_\rho A_0^{B\rho}(m_D^2), \end{aligned} \quad (65)$$

while E is again negligible. For $\overline{B}^0 \rightarrow D^0\omega$ one has

$$A_{D^0\omega}^f = \frac{G_F}{\sqrt{2}} V_{cb} V_{ud}^* a_2 f_D 2m_\omega A_0^{B\omega}(m_D^2). \quad (66)$$

We set $A_{D_s^+ K^{*-}}^f = A_{D^0\phi}^f = 0$ for the factorization amplitudes of $\overline{B}^0 \rightarrow D_s^+ K^{*-}$, $D^0\phi$ modes. We again normalize to $D^0\rho^-$ mode since its rate is unaffected by FSI. We take the $D^0\omega$ measurement from Ref. [1], while the measurements of $D^+\rho^-$, $D^0\rho^-$ modes and the upper limit of $\mathcal{B}(D^0\rho^0)$ are taken from PDG [3].

Because of the reduction to one phase difference for both Solution 1 and Solution 2 of Eqs. (55) and (56), we are able to fit with just $D^+\rho^-$ and $D^0\omega$ data. We find δ' (σ) to be 18° (35°) for Solution 1 (Solution 2), as given in Table IV. Since the FSI contributions to $D^0\rho^0$ and $D^0\omega$ are mainly fed from $D^+\rho^-$ and $A_{D^0\rho^0}^f \approx -A_{D^0\omega}^f$, Eq. (57) leads to

$$\begin{aligned} A_{D^0\rho^0(\omega)} &\approx \frac{i(r'_a \mp r'_e)}{\sqrt{2}} A_{D^+\rho^-}^f + (1 + ir'_0) A_{D^0\omega}^f \\ &\approx \frac{i(r'_a \mp r'_e)}{\sqrt{2}} A_{D^+\rho^-}^f \mp (1 + ir'_0) A_{D^0\omega}^f, \end{aligned} \quad (67)$$

where r'_0 , r'_a and r'_e are defined in Sec. IV.B. For Solution 1 (Solution 2) the dominant FSI contributions to $D^0\rho^0$ and $D^0\omega$ are the same in magnitude but opposite (same) in sign due to r'_e (r'_a) $\neq 0$. This implies different interference patterns. For Solution 1, we have $\mathcal{B}(D^0\rho^0) \sim \mathcal{B}(D^0\omega)$. For Solution 2, since $A_{D^+\rho^-}^f$ and $A_{D^0\omega}^f$ are real and of same sign,

$$\begin{aligned} (1 + ir'_0)e^{-i\delta_{3/2}} &= 1, \\ \text{Re}(ir'_a e^{-i\delta_{3/2}}) &= \frac{1}{3}[\cos \sigma - 1] \leq 0, \end{aligned} \quad (68)$$

TABLE IV: The best fit phase difference for DV modes.

Mode	Solution 1	Solution 2
χ^2	1.20	0.64
δ'	18.1°	—
σ	—	34.8°
$(1 + ir_0)e^{-2i\delta_{3/2}}$	$0.90 + 0.30i$	1
$ir_e e^{-2i\delta_{3/2}}$	$0.10 - 0.30i$	0
$ir_a e^{-2i\delta_{3/2}}$	0	$-0.22 + 0.31i$

TABLE V: The branching ratios of various DV modes. The second and third columns compare experiment with factorization model. The last two columns give the best fit results with FSI parameters of Table IV.

Mode	$\mathcal{B} (\times 10^{-4})$	fac ^{LF (NS)}	Solution 1	Solution 2
$D^+\rho^-$	79 ± 18	100.7 (101.2)	98.2	92.7
$D^0\omega$	1.8 ± 0.5 $^{+0.4}_{-0.3}$	0.67 (0.64)	1.86	1.92
$D^0\rho^0$	< 3.9	0.67 (0.64)	1.90	3.37
$D_s^+ K^{*-}$	< 9.9	0	0	2.73
$D^0\phi$	—	0	0	0

the FSI contribution always interferes destructively (constructively) with $A_{D^0\omega}^f$ ($A_{D^0\rho^0}^f$). While $\mathcal{B}(D^0\rho^0)$ becomes larger, one would need large annihilation contribution to account for the observed $D^0\omega$ data, which in turn gives rise to $\mathcal{B}(D_s^+ K^{*-})$ as large as 2.7×10^{-4} . These patterns can be tested in the near future.

On the other hand, $D^0\phi$ only rescatters with $D_s^+ K^{*-}$, as can be seen from Eqs. (57). It does not pick up any FSI contribution since $A_{D_s^+ K^{*-}}^f = 0$, even if $A_{D_s^+ K^{*-}}$ is nonvanishing as in the Solution 2 case. Observation of $D^0\phi$ mode would imply some mechanism at the “source” level. Our fitted branching ratios and predictions for various PV modes are given in Table V.

We note that $|A_{1/2}/(\sqrt{2}A_{3/2})| = 0.84$, $|\delta_{1/2} - \delta_{3/2}| = 12.7^\circ$ from Solution 1 and $|A_{1/2}/(\sqrt{2}A_{3/2})| = 0.81$, $|\delta_{1/2} - \delta_{3/2}| = 18.5^\circ$ from Solution 2. The phase angles are somewhat smaller than those for $D^{(*)}\pi$ modes.

C. Predictions for $D^{(*)}\overline{K}$ and $D\overline{K}^*$ Modes

Our FSI formulas can be applied readily to rescattering between the Cabibbo suppressed modes, $D^{(*)+}K^-$ and $D^{(*)0}K^0$, since they are contained in the formalism for $D^{(*)}P$. Following similar procedure as before, we have

$$2 \begin{pmatrix} \text{Im } A_{D^{(*)+}K^-} \\ \text{Im } A_{D^{(*)0}K^0} \end{pmatrix} = \mathcal{T}^\dagger \begin{pmatrix} A_{D^{(*)+}K^-} \\ A_{D^{(*)0}K^0} \end{pmatrix}, \quad (69)$$

where

$$\mathcal{T} = \begin{pmatrix} r_0 & r_e \\ r_e & r_0 \end{pmatrix}, \quad (70)$$

and “annihilation” is clearly impossible as can be seen from the pictorial approach. By using Eq. (37), we note that $\mathcal{S} = \mathbf{1} + i\mathcal{T}$ is automatically unitary. Therefore, we obtain

$$\begin{pmatrix} A_{D^{(*)+}K^-} \\ A_{D^{(*)0}K^0} \end{pmatrix} = \mathcal{S}^{1/2} \begin{pmatrix} A_{D^{(*)+}K^-}^f \\ A_{D^{(*)0}K^0}^f \end{pmatrix}, \quad (71)$$

where,

$$\mathcal{S}^{1/2} = \frac{e^{i\delta_{3/2}}}{2} \begin{pmatrix} 1 + e^{i\delta'} & 1 - e^{i\delta'} \\ 1 - e^{i\delta'} & 1 + e^{i\delta'} \end{pmatrix}, \quad (72)$$

TABLE VI: The predicted branching ratios of $D^{(*)}\bar{K}$ and $D\bar{K}^*$ modes in 10^{-4} units. The second and third columns compare experiment with factorization model. The last three columns give the best fit results with FSI parameters of Table II and Table IV.

Mode	$\mathcal{B} (\times 10^{-4})$	fac ^{LF}	Fit1 _{DP}	Fit _{D*P}	Solution 1
$D^0 K^-$	4.2 ± 0.7	4.12	—	—	—
$D^+ K^-$	2.0 ± 0.6	2.61	2.20	—	—
$D^0 \bar{K}^0$	—	0.12	0.53	—	—
$D^{*0} K^-$	3.6 ± 1.0	3.40	—	—	—
$D^{*+} K^-$	2.0 ± 0.5	2.15	—	1.71	—
$D^{*0} \bar{K}^0$	—	0.10	—	0.55	—
$D^0 K^{*-}$	—	7.0	—	—	—
$D^+ K^{*-}$	—	5.11	—	—	4.99
$D^0 \bar{K}^{*0}$	—	0.09	—	—	0.21

which is consistence with those obtained in Appendix A, and the factorization amplitudes are

$$\begin{aligned}
 A_{D+K^-}^f &= \frac{G_F}{\sqrt{2}} V_{cb} V_{us}^* a_1 (m_B^2 - m_D^2) f_K F_0^{BD}(m_K^2), \\
 A_{D^0 \bar{K}^0}^f &= \frac{G_F}{\sqrt{2}} V_{cb} V_{us}^* a_2 (m_B^2 - m_{K^0}^2) f_D F_0^{BK}(m_{D^0}^2), \\
 A_{D^{*+} K^-}^f &= \frac{G_F}{\sqrt{2}} V_{cb} V_{us}^* a_1 2m_{D^*} f_K A_0^{BD}(m_K^2), \\
 A_{D^{*0} \bar{K}^0}^f &= \frac{G_F}{\sqrt{2}} V_{cb} V_{us}^* a_2 2m_{D^*} f_D F_1^{BK}(m_{D^{*0}}^2), \quad (73)
 \end{aligned}$$

where form factors are found in Table I. One again has a triangle relation $A_{D^{(*)0} K^-}^f = A_{D^{(*)+} K^-}^f + A_{D^{(*)0} \bar{K}^0}^f$.

The δ' phase has already been fitted, and the predicted branching ratios for $D\bar{K}$ and $D^*\bar{K}$ modes are given in Table VI. The second column is obtained by multiplying Belle measurements of $\mathcal{B}(D^{*,0} K^-)/\mathcal{B}(D^{*,0} \pi^-)$ [20] by PDG values of $\mathcal{B}(D^{*,0} \pi^-)$ [3].

It is interesting to note that $D^{(*)}\bar{K}$ modes do not receive the annihilation type FSI, r_a , and the \bar{K}^0 wave function does not have the $1/\sqrt{2}$ factor as compared to π^0 . For “Fit1_{DP}” and “Fit_{D*P}”, r_a is subdominant while $|r_e|$ is close to each other, hence we find that $\mathcal{B}(D^0 \bar{K}^0)/\mathcal{B}(D^+ K^-) \approx 2\mathcal{B}(D^0 \pi^0)/\mathcal{B}(D^+ \pi^-) \approx 2 \times 1/10$ and $\mathcal{B}(D^{*0} \bar{K}^0) \approx \mathcal{B}(D^0 K^0)$. As noted, “Fit2_{DP}” is ruled out already by $D_s^+ K^-$ bound.

In a very similar fashion, we predict the rescattering of $D^+ K^{*-}$ into $D^0 \bar{K}^{*0}$ final state, which is given again in Table VI for Solution 1 of DV case, where one again has $\mathcal{B}(D^0 \bar{K}^{*0})/\mathcal{B}(D^+ K^{*-}) \approx 2\mathcal{B}(D^0 \rho^0)/\mathcal{B}(D^+ \rho^-) \approx 2 \times 1/50$. For Solution 2, $r_e = 0$ and the result is the same as the second column for factorization.

The $D\bar{K}^*$ modes have yet to be observed. The factorization predictions for $D^0 K^{*-}$ and $D^+ K^{*-}$ are about twice as large as $D^{*0} K^-$ and $D^{*+} K^-$, but the predicted branching ratio for $\bar{B} \rightarrow D^0 \bar{K}^{*0}$ is less than half of $\bar{B} \rightarrow D^{*0} \bar{K}^0$ in Solution 1. This is because $|r_e|$ (or the rescattering phase δ') for DV modes are much smaller than for D^*P modes. We note that in Solution 2 one

would predict $\bar{B} \rightarrow D^0 \bar{K}^{*0}$ to occur at half the rate of the Solution 1 case, i.e. just the factorization a_2 prediction.

Our formalism therefore predicts a relatively sizable $\mathcal{B}(D^{(*)0} \bar{K}^0)$ at $\sim 0.5 \times 10^{-4}$, and expect $\mathcal{B}(D^0 \bar{K}^{*0}) \sim 0.2 \times 10^{-4}$ (0.1×10^{-4} if Solution 2 is confirmed). We encourage Belle and BaBar to search for these modes.

VI. DISCUSSION AND CONCLUSION

We have stressed that the isospin relation of Eq. (13), which follows from Eq. (1) (given more explicitly in Eqs. (9)–(11)), holds whether one has FSI or not. This was used to extract $A_{1/2}/A_{3/2}$ directly from $D^{(*)}\pi$ data, as given in Eq. (15), which we reproduce here:

$$\begin{aligned}
 \frac{1}{\sqrt{2}} \left| \frac{A_{1/2}}{A_{3/2}} \right|^{D^{(*)}\pi \text{ only}} &= 0.71 \pm 0.11 \quad (0.75 \pm 0.08), \\
 |\delta|^{D^{(*)}\pi \text{ only}} &= 29^\circ \pm 6^\circ \quad (30^\circ \pm 7^\circ), \quad (74)
 \end{aligned}$$

where it is made clear that they are extracted from $D^{(*)}\pi$ data alone. On the other hand, we have given in Table II the values for $|A_{1/2}/(\sqrt{2}A_{3/2})|$ and $|\delta_{1/2} - \delta_{3/2}|$ as obtained by using the fitted strong phases that takes into account $D^0 \eta^{(*)0}$ data, i.e. by using the $A_{D^{(*)0} \pi^-}$, $A_{D^{(*)+} \pi^-}$ and $A_{D^{(*)0} \pi^0}$ amplitudes of Eq. (39). They turn out to be not so different from Eq. (74). Let us understand why.

We note that $|A_{1/2}/(\sqrt{2}A_{3/2})| = 1 + \mathcal{O}(\Lambda/m_Q) \rightarrow 1$ in the heavy b (and c) quark limit [5, 7], although m_c may not be heavy enough. The strong phase $|\delta_{1/2} - \delta_{3/2}| \rightarrow 0$ in the absence of short and long distance rescattering. It is instructive to consider first the elastic $D^{(*)}\pi \rightarrow D^{(*)}\pi$ rescattering case. Noting that elastic rescattering does not change $|A_I|$ from its factorization value, for $D^{(*)}P$ modes we have, roughly speaking,

$$\frac{|A_{1/2}|}{\sqrt{2}|A_{3/2}|} = \frac{|A_{1/2}^f|}{\sqrt{2}|A_{3/2}^f|} = \frac{|2T - C|}{2|T + C|} \sim \frac{|2 - \frac{a_2}{a_1}|}{2|1 + \frac{a_2}{a_1}|}, \quad (75)$$

which deviates from 1 due to a nonzero a_2 , which is a nonfactorizable effect. It was a happy coincidence, before the measurement of color-suppressed modes, that taking $a_2/a_1 = 0.25$ and *real* could account for [4] both $B^- \rightarrow D^0 \pi^-$ and $\bar{B} \rightarrow J/\psi \bar{K}^{(*)}$ rates. It should be stressed that the sizable value of $|a_2/a_1|$ can be viewed as determined this way from data that gives $|A_{1/2}/(\sqrt{2}A_{3/2})| \simeq 0.7$.

The impact of the new experimental measurement of $D^0 \pi^0$ is that one is now able to determine the strong phase difference, $|\delta_{1/2} - \delta_{3/2}| \sim 30^\circ$, which is not quite small. With this one has two ways to proceed.

As mentioned in the Introduction, Refs. [7, 8] continue to employ factorization formulas to $D^{(*)0} \pi^0$ hence make $|a_2|$ larger by roughly *a factor of two*. To maintain $D^{(*)0} \pi^-$ and generate $\delta_{1/2} - \delta_{3/2}$, one capitalizes on Eq. (75) by dropping the absolute value condition. That

is, one resorts to a complex a_2/a_1 itself. In this way one finds $|a_2| \sim 0.4\text{--}0.5$ and $\arg a_2 \sim 60^\circ$ could account for $\overline{B} \rightarrow D\pi$ data, at the cost that $|a_2|$ is twice as large as from $J/\psi\overline{K}^{(*)}$ modes. Ref. [7] argues further that, while factorization no longer holds, the trend of larger and complex a_2 is expected from QCD factorization [5].

Our critique is the following. First, this “ a_2 ” approach is process dependent, and predictiveness is lost. Although $|a_2| \sim 0.4\text{--}0.5$ could account for the strength of observed $D^{(*)0}\eta$ and $D^{(*)0}\omega$ modes, it seems coincidental, with $|a_2|$ varying by $\sim 20\text{--}30\%$ among these and $D^{(*)0}\pi^0$ modes, while we know that $|a_2| \sim 0.2\text{--}0.3$ for $J/\psi\overline{K}^{(*)}$ modes. Second, it is the need to maintain $D^{(*)0}\pi^-$ rate that a sizable phase to a_2 is invoked, although previously a smaller and real a_2 gave a pleasant, consistent picture. However, from Eq. (75) we know that a_2 reduces $|A_{1/2}/(\sqrt{2}A_{3/2})|$ hence it represents *inelastic* effects [21]. This is the reason why it is not quite calculable. In this sense, however, $\arg a_2 \sim 60^\circ$ is not reasonable since one expects strong cancellations among numerous inelastic channels [9, 12]. A statistical model suggests the typical phase to be $\sim 20^\circ$ [9]. Third, we stress that generating Eq. (74) by the phase and strength of a_2 holds only when one drops the absolute value requirement from Eq. (75), i.e. ignoring elastic FSI, as is common practice in QCD factorization [5]. Such FSI effects are $\mathcal{O}(\alpha_s(m_b))$ suppressed, or $1/m_Q$ suppressed. For the former, clearly $\alpha_s(m_b) \sim 0.2 \sim 10^\circ$ in radians. For the latter, one has the real problem that m_c may *not* be heavy enough.

The approach advocated in this paper is via quasi-elastic FSI rescattering. Let’s make a point by point comparison with the “process dependent a_2 ” approach. First, process independence is not so easily conceded. In particular, we maintain $a_2/a_1 \cong 0.25$ and real. Thus, the proximity of Eq. (75) with Eq. (74) reflects a phenomenological tuning done several years ago. The philosophy is that, while we agree that a_2 should be process dependent and in principle complex, we take the above “tuned” value as no mere accident. That is, Nature could have revealed to us long ago that a_2 is strongly process dependent. Since keeping both a_2 as parameter *and* allowing for FSI phases cannot lead one afar, we opt to keep a_2/a_1 fixed as done in [4]. The new experimental measurement of $D^{(*)0}\eta$ and $D^{(*)0}\omega$ modes, rather than giving “process dependence” irritation, can be incorporated nicely by enlarging the scope of FSI from elastic SU(2) to quasi-elastic SU(3) symmetry. This stretching of “elasticity”, together with maintaining process independence to good degree, make our approach suitably predictive. Second, by leaving a_2/a_1 as done before in [4], one enjoys the success with $D^0\pi^-/D^+\pi^-$ and $J/\psi\overline{K}$. The strength of a_2 is smaller, hence the acuteness of inelasticity is not as severe as the “ a_2 ” approach. A strong phase of order 50° does emerge, but this is interpreted as due to having $D^{(*)0}\pi^0$ and $D^{(*)0}\eta$ both sizable (see Appendix B), and has completely different origins from the need for $\arg a_2 \sim 60^\circ$ in the large “ a_2 ” approach. Finally, in comparison with the strong assumption of re-

moving the absolute value condition from Eq. (75), we took advantage of FSI approach to expand a previously commonly known “folklore” on elastic FSI rescattering.

We can now comment on comparison of Eq. (74) with values in Table II. With $a_2/a_1 = 0.25$, we find $|A_{1/2}/(\sqrt{2}A_{3/2})| = |A_{1/2}^f/(\sqrt{2}A_{3/2}^f)| = 0.77$ (0.75) for LF and 0.77 (0.73) for NS form factors. Assuming elastic rescattering and using the formulas of Sec. III, the strength of amplitudes cannot change, and we find $|\delta_{1/2} - \delta_{3/2}| = 30.6^\circ$ (29.9°) for LF and 30.6° (29.2°) for NS form factors. Note that the form factor dependence is very weak. With rescattering among SU(3) multiplets, $A_{1/2}^f$ can now feed other color suppressed modes via rescattering (Eq. (45)). The $D^{(*)0}\pi^-$ mode still can not rescatter to other modes, so $|A_{3/2}| = A_{3/2}^f = |A_{D^0\pi^-}|/\sqrt{3}$. Thus, from unitarity we expect $|A_{1/2}/A_{3/2}| < |A_{1/2}^f/A_{3/2}^f|$ in the presence of quasi-elastic FSI. We see from Table II that $|A_{1/2}/A_{3/2}|$ is reduced from the factorization results by 3%, 16% respectively, for Fit1_{DP}, Fit2_{DP}, and by 5% for Fit_{D*P}. Except the second case, which is ruled out by $\overline{B}^0 \rightarrow D_s^+ K^-$ data, the deviation from elastic FSI is mild. This reflects the fact that the color-suppressed $D^{(*)0}\eta$ rate is still small compared to $D^{(*)+}\pi^-$. The strong phases $|\delta_{1/2} - \delta_{3/2}|$ in Table II agree rather well with the directly extracted ones (Eq. (74)) as well as the elastic ones, and the validity of Eq. (46) as good estimates is born out.

A principle motivation and interest in understanding color-suppressed $\overline{B} \rightarrow D^{(*)0}h^{(*)0}$ modes is its possible implication for $\overline{B} \rightarrow \overline{K}\pi$ and $\pi\pi$ final states. These modes have been one of the focal points in B physics in recent years, because it provides rich probes of CP violation [22] and possibilities [23] for new physics. We note that the effect of a_2 is rather subdued in these processes, but our picture of rescattering may still be realized, hence these processes provide more fertile testing ground for FSI. Effects of FSI rescattering on $K\pi$, $\pi\pi$ final states have been discussed in the literature [9, 12, 18, 24]. In particular, it has been stressed [25] that large rescattering phases in $\overline{K}\pi \rightarrow \overline{K}\pi$ and $\pi\pi \rightarrow \pi\pi$ could have dramatic impact on such charmless final states. If phases analogous to $\delta' \sim 50^\circ$ can be realized, the $\overline{K}^0\pi^0$ and $\pi^0\pi^0$ modes could get enhanced while $\pi^+\pi^-$ mode suppressed. Direct CP rate asymmetries could soon be observed in $\overline{K}\pi$ modes, in particular in “pure penguin” $\overline{K}^0\pi^-$ mode, while for $\pi^0\pi^0$ and $\pi^+\pi^-$ modes they could even reach 50–60%. The formalism is a straightforward extension from the one presented here. Rather than DII \rightarrow DII rescattering, one now needs to study III \rightarrow III rescattering. It is interesting to note that the factorization “sources” for all four $\overline{K}\pi$ modes are sizable, unlike our present case where the $D^+\pi^-$ mode is the singly large source. Thus, the cross-feed between channels would be different. Furthermore, the CP violating rate asymmetries provide additional leverage to check for the presence of FSI phases. In this sense the $K\pi$, $\pi\pi$ (PP in broader sense) system is richer than our present $D^{(*)}P$ case. It is interesting

that the physical picture of r_i is still applicable with an additional annihilation rescattering term, due to possible final states consist of $P\bar{P}$. Our study is underway and would be reported elsewhere.

Finally, we mention a curiosity. Fit2_{DP} contains large “annihilation” rescattering, which runs against $\bar{B}^0 \rightarrow D_s^+ K^-$ data hence is ruled out. Fit1_{DP} and Fit_{D*P}, as well as Solution 1 of DV case, all had exchange rescattering far dominant over annihilation. Thus, Solution 2 of DV case is the only one where the latter is sizable and dominant. It therefore has the distinct feature that $D^0\rho^0$ is almost twice as large as $D^0\omega$, with $D_s^+K^-$ not much smaller. However, if this were realized, then one would expect $\bar{B}^0 \rightarrow D^0\bar{K}^{*0}$ to be at factorization rate and much weaker than $D^0\bar{K}^0$ and $D^{*0}\bar{K}^0$, which would be rather peculiar. We would therefore not be surprised if Solution 2 gets ruled out soon, and one might then conclude that rescattering is largely in terms of the classic “charge exchange” type. This may also explain why $K\bar{K}$ modes are so far unseen. In this vein we wish to remark also that we have not exhausted the predictive-ness of our approach. For instance, one could generate “wrong charge” $\bar{B} \rightarrow \bar{D}^0\bar{K}$ decays via $D_s^-\pi^0 \rightarrow \bar{D}^0K^-$ and $D_s^-\pi^+ \rightarrow \bar{D}^0\bar{K}^0$ rescattering from V_{ub} suppressed $\bar{B} \rightarrow D_s^-\pi^0, D_s^-\pi^+$ decays. The rescattering matrix can be adapted from results presented here, but the latter decays have yet to be observed.

In conclusion, we advocate in this work the possibility that the recently observed host of $\bar{B} \rightarrow D^0h^0$ modes may be hinting at final state rescattering. In contrast to a sug-

gestion of a larger and complex a_2 , we extend the elastic $D^{(*)}\pi \rightarrow D^{(*)}\pi$ FSI picture to quasi-elastic $D^{(*)}P \rightarrow D^{(*)}P$ and $DV \rightarrow DV$ rescattering, where P is the pseudoscalar SU(3) octet, and V is the vector U(3) nonet. In this way we are able to accommodate $D^{(*)0}\eta, D^0\omega$ modes in a unified setting. For $D^{(*)}P$ modes, we find that data give rise to two rescattering phases $\delta' \sim 50^\circ$ and $\theta \sim 20^\circ$, where the need for a large phase comes about because of the strength of *both* the $D^{(*)0}\pi^0$ and $D^{(*)0}\eta$ modes. For DV modes, nonet symmetry reduces the number of physical phases to one, of order $20\text{--}30^\circ$. The emerging pattern is that of “charge exchange” rescattering, rather than “quark annihilation”. We predict rather small $\bar{B}^0 \rightarrow D_s^{(*)+}K^-, D_s^+K^{(*)-}$ and $D^0\phi$ rates, and $D^0\rho^0 \simeq D^0\omega$, although in one solution one could have $D^0\rho^0 \simeq 2 \times D^0\omega$ and $\bar{B}^0 \rightarrow D_s^+K^{(*)-} \sim 3 \times 10^{-4}$, which can be easily checked. We expect $\bar{B}^0 \rightarrow D^{(*)0}\bar{K}^0$ and $D^0\bar{K}^{*0}$ to be at 0.55×10^{-4} and 0.2×10^{-4} , respectively, which is sizable. While these predictions can be tested experimentally, the $K\pi, \pi\pi$ charmless final states are even more promising, if FSI phases are as large as 50° , because one then expects rather sizable direct CP asymmetries with a distinct pattern.

Acknowledgments

This work is supported in part by the National Science Council of R.O.C. under Grants NSC-90-2112-M-002-022, NSC-90-2811-M-002-038 and NSC-90-2112-M-033-004, the MOE CosPA Project, and the BCP Topical Program of NCTS.

APPENDIX A: SU(3) DECOMPOSITION OF THE RESCATTERING MATRIX

It is well known that $D^{0,+}, D_s^+$ and π, K, η transform respectively as $\bar{\mathbf{3}}$ and $\mathbf{8}$ under SU(3),

$$\bar{D}(\bar{\mathbf{3}}) = (D^0 \ D^+ \ D_s^+), \quad \Pi(\mathbf{8}) = \begin{pmatrix} \frac{\pi^0}{\sqrt{2}} + \frac{\eta_8}{\sqrt{6}} & \pi^+ & K^+ \\ \pi^- & -\frac{\pi^0}{\sqrt{2}} + \frac{\eta_8}{\sqrt{6}} & K^0 \\ K^- & \bar{K}^0 & -\sqrt{\frac{2}{3}}\eta_8 \end{pmatrix}. \quad (\text{A1})$$

The $\bar{D}(\bar{\mathbf{3}}) \otimes \Pi(\mathbf{8})$ can be reduced into a $\bar{\mathbf{3}}$, a $\mathbf{6}$ and a $\bar{\mathbf{15}}$, i.e. (see for example, [13])

$$\begin{aligned} T(\bar{\mathbf{3}})_j &\equiv \bar{D}_l \Pi_j^l, \quad T(\mathbf{6})^{li} \equiv \epsilon^{lmn} \bar{D}_m \Pi_n^i + \epsilon^{imn} \bar{D}_m \Pi_n^l, \\ T(\bar{\mathbf{15}})_{jk}^i &\equiv \bar{D}_k \Pi_j^i + \bar{D}_j \Pi_k^i - \frac{1}{4} \delta_k^i \bar{D}_l \Pi_j^l - \frac{1}{4} \delta_j^i \bar{D}_l \Pi_k^l. \end{aligned} \quad (\text{A2})$$

The SU(3) symmetry of strong interaction enforces the twenty-four by twenty-four scattering matrix having the following form

$$\mathcal{S}^{1/2} = e^{i\delta_{\bar{\mathbf{15}}}} \sum_{a=1}^{15} |T(\bar{\mathbf{15}}); a\rangle \langle T(\bar{\mathbf{15}}); a| + e^{i\delta_6} \sum_{b=1}^6 |T(\mathbf{6}); b\rangle \langle T(\mathbf{6}); b| + e^{i\delta_{\bar{\mathbf{3}}}} \sum_{c=1}^3 |T(\bar{\mathbf{3}}); c\rangle \langle T(\bar{\mathbf{3}}); c|; \quad (\text{A3})$$

where $|T(\bar{\mathbf{15}}); a\rangle, |T(\mathbf{6}); b\rangle$ and $|T(\bar{\mathbf{3}}); c\rangle$ are orthonormal SU(3) basis for the irreducible representations shown in the above equation.

Although the twenty-four by twenty-four rescattering matrix is diagonal in these basis, we may not need all of them in a realistic situation. For a final state with given strangeness and isospin (or electric charge) it can only rescatter to other final states having same quantum numbers. For later purpose, we give the explicit forms of these basis. By proper linear combining states within the same multiple, as shown in Eq. (A2), $|T(\overline{15}); a\rangle$ can be classified according to strangeness (S) and isospin (I)

$$(S = 1, I = 1) : \frac{|D^+K^+ \rangle + |D_s^+\pi^+ \rangle}{\sqrt{2}}, \frac{|D^+K^0 \rangle - |D^0K^+ \rangle - \sqrt{2}|D_s^+\pi^0 \rangle}{2}, \frac{|D^0K^0 \rangle + |D_s^+\pi^- \rangle}{\sqrt{2}}; \quad (\text{A4})$$

$$(S = 1, I = \frac{1}{2}) : |D_s^+K^+ \rangle, |D_s^+K^0 \rangle; \quad (\text{A5})$$

$$(S = 1, I = 0) : \frac{|D^+K^0 \rangle + |D^0K^+ \rangle + \sqrt{6}|D_s^+\eta_8 \rangle}{2\sqrt{2}}. \quad (\text{A6})$$

$$(S = 0, I = \frac{3}{2}) : |D^+\pi^+ \rangle, \frac{1}{3}|D^0\pi^+ \rangle + \sqrt{\frac{2}{3}}|D^+\pi^0 \rangle, \frac{1}{\sqrt{3}}|D^+\pi^- \rangle - \sqrt{\frac{2}{3}}|D^0\pi^0 \rangle, |D^0\pi^- \rangle; \quad (\text{A7})$$

$$(S = 0, I = \frac{1}{2}) : \frac{2|D^0\pi^+ \rangle - \sqrt{2}|D^+\pi^0 \rangle + 3\sqrt{6}|D^+\eta_8 \rangle - 6|D_s^+\overline{K}^0 \rangle}{4\sqrt{6}}, \quad (\text{A8})$$

$$\frac{2|D^+\pi^- \rangle + \sqrt{2}|D^0\pi^0 \rangle + 3\sqrt{6}|D^0\eta_8 \rangle - 6|D_s^+K^- \rangle}{4\sqrt{6}}; \quad (\text{A9})$$

$$(S = -1, I = 1) : |D^+\overline{K}^0 \rangle, \frac{|D^+K^- \rangle + |D^0\overline{K}^0 \rangle}{\sqrt{2}}, |D^0K^- \rangle. \quad (\text{A10})$$

Similarly $|T(6), b\rangle$ are

$$(S = 1, I = 1) : \frac{|D^+K^+ \rangle - |D_s^+\pi^+ \rangle}{\sqrt{2}}, \frac{|D^+K^0 \rangle - |D^0K^+ \rangle + \sqrt{2}|D_s^+\pi^0 \rangle}{2}, \frac{|D^0K^0 \rangle - |D_s^+\pi^- \rangle}{\sqrt{2}}, \quad (\text{A11})$$

$$(S = 0, I = \frac{1}{2}) : \frac{2|D^0\pi^+ \rangle - \sqrt{2}|D^+\pi^0 \rangle - \sqrt{6}|D^+\eta_8 \rangle - 2|D_s^+\overline{K}^0 \rangle}{4}, \frac{2|D^+\pi^- \rangle + \sqrt{2}|D^0\pi^0 \rangle - \sqrt{6}|D^0\eta_8 \rangle - 2|D_s^+K^- \rangle}{4}, \quad (\text{A12})$$

$$(S = -1, I = 0) : \frac{|D^+K^- \rangle - |D^0\overline{K}^0 \rangle}{\sqrt{2}}. \quad (\text{A13})$$

The $|T(\overline{3}), c\rangle$ are

$$(S = 0, I = 1/2) : \frac{6|D^0\pi^+ \rangle - 3\sqrt{2}|D^+\pi^0 \rangle + \sqrt{6}|D^+\eta_8 \rangle + 6|D_s^+\overline{K}^0 \rangle}{4\sqrt{6}}, \frac{6|D^+\pi^- \rangle + 3\sqrt{2}|D^0\pi^0 \rangle + \sqrt{6}|D^0\eta_8 \rangle + 6|D_s^+K^- \rangle}{4\sqrt{6}}, \quad (\text{A14})$$

$$(S = 1, I = 0) : \frac{3|D^+K^0 \rangle + 3|D^0K^+ \rangle - \sqrt{6}|D_s^+\eta_8 \rangle}{2\sqrt{6}}. \quad (\text{A15})$$

With these basis, it is then straightforward to obtain $\mathcal{S}^{1/2}$ by using Eq. (A3). As noted before we only need final states with same quantum numbers for rescattering. For example, $I = 3/2$ states can only appear in $\overline{15}$, hence we identify $\delta_{3/2}$ as $\delta_{\overline{15}}$. For $S = -1$ and $Q = 0$, we only have $D^0\overline{K}^0$ and D^+K^- for rescattering. By using two neutral and $S = -1$ states in $\overline{15}$ and 6, respectively, we immediately obtain $\mathcal{S}^{1/2}$ in Eq. (71). Similarly, by using $S = Q = 0$, $I = 3/2, 1/2$ states in $\overline{15}$ and $I = 1/2$ states in 6 and $\overline{3}$, we obtain $\mathcal{S}^{1/2}$ in Eq. (40) readily.

We now turn to the DV case. The $SU(3)$ decomposition of DV final states can be obtained by replacing π , K and η_8 in the DP case by ρ , K^* and ω_8 , respectively. However, there is another $\overline{3}$ as $|T(\overline{3}'); i\rangle = |\overline{D}(\overline{3})_i\omega_1\rangle$. This $\overline{3}'$ can mix with the previous $\overline{3}$ with a two by two symmetric (due to time reversal invariant) unitary matrix $\mathcal{U}^{1/2}$. We have

$$\mathcal{S}_V^{1/2} = e^{i\delta_{\overline{15}}} \sum_{a=1}^{15} |T(\overline{15}); a\rangle \langle T(\overline{15}); a| + e^{i\delta_6} \sum_{b=1}^6 |T(6); b\rangle \langle T(6); b| + \sum_{m,n=\overline{3},\overline{3}'} \sum_{c=1}^3 |T(m); c\rangle \mathcal{U}_{mn}^{1/2} \langle T(n); c|, \quad (\text{A16})$$

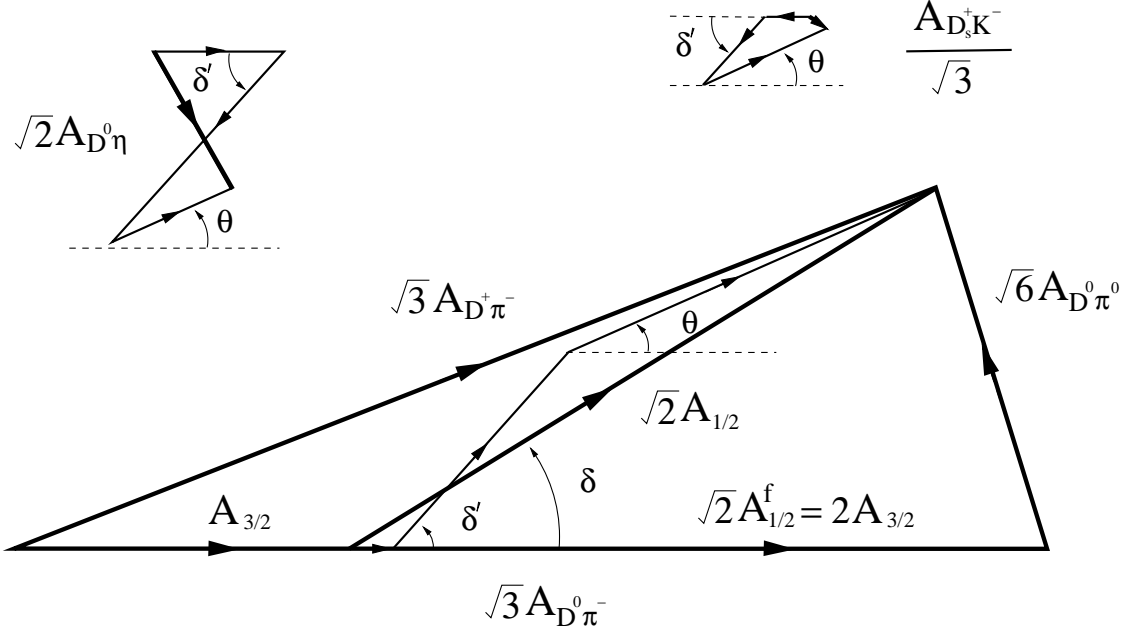


FIG. 5: Geometric representation of $\overline{B} \rightarrow DP$ rescattering of Eq. (B1).

for DV rescattering matrix. Note that the symmetric mixing matrix $\mathcal{U}^{1/2}$ can be parametrized by two phases and one mixing angle. We need four parameters, including three phase differences and one mixing angle, to describe the DV FSI case. On the other hand by nonet symmetry we reduce them to only one parameter (in addition to an overall phase) but with two distinct solutions as discussed in Section IV.

APPENDIX B: GEOMETRIC REPRESENTATION

We give the geometric (triangular) representation of our results in this Appendix. For simplicity of presentation, we consider the leading FSI contribution and drop the a_2 contribution. The triangular relation for the $D\pi$ system, Eqs. (9) and (10), and the FSI formula for $D^0\eta$, $D_s^+K^-$, Eqs. (44) and (45), will then be reduced to

$$\begin{aligned}
\sqrt{3}A_{D^+\pi^-} &= A_{3/2} + \sqrt{2}A_{1/2}, & \sqrt{2}A_{1/2} &= \frac{1}{16}(1 + 6e^{i\delta'} + 9e^{i\theta})(\sqrt{2}e^{i\delta_{3/2}}A_{1/2}^f), \\
\sqrt{6}A_{D^0\pi^0} &= -2A_{3/2} + \sqrt{2}A_{1/2}, & \sqrt{2}A_{D^0\eta} &= \frac{1}{16}(3 - 6e^{i\delta'} + 3e^{i\theta})(\sqrt{2}e^{i\delta_{3/2}}A_{1/2}^f), \\
\sqrt{3}A_{D^0\pi^-} &= 3A_{3/2}, & \frac{A_{D_s^+K^-}}{\sqrt{3}} &= \frac{1}{16}(-1 - 2e^{i\delta'} + 3e^{i\theta})(\sqrt{2}e^{i\delta_{3/2}}A_{1/2}^f), \\
A_{3/2} &= e^{i\delta_{3/2}}A_{3/2}^f, & \sqrt{2}A_{1/2}^f &= 2A_{3/2}^f,
\end{aligned} \tag{B1}$$

where the last equation follows from $\sqrt{6}A_{D^0\pi^0}^f = -2A_{3/2}^f + \sqrt{2}A_{1/2}^f = 0$ when $a_2 = 0$. Eq. (13) still holds, and $|A_{3/2}| = |A_{3/2}^f|$, but we now have $|A_{1/2}| \leq |A_{1/2}^f|$ due to quasi-elastic rescattering.

We illustrate the amplitudes of Fit1_{DP} , i.e. $\delta' = 47.8^\circ$ and $\theta = 24.8^\circ$, in Fig. 5. The D^*P case is similar. We have chosen the x -axis to coincide with $A_{3/2}$. Since δ' and θ are of the same sign, when considering only $D^0\pi^0$, there is no need for a large angle, and $\delta' \sim \theta \sim \delta = \delta_{1/2} - \delta_{3/2} \sim 30^\circ$ would have been good enough. However, because θ has same sign as δ' , as we can see from Fig. 5, the third phaser contributing to $A_{D^0\eta}$, i.e. $3e^{i\theta}/16(e^{i\delta_{3/2}}\sqrt{2}A_{1/2}^f)$, turns back and tends to reduce $\sqrt{2}A_{D^0\eta}$. We therefore need to start with a larger δ' to compensate. Thus, the relatively large phase $\delta' \sim 50^\circ$ is driven by the strength of the measured $\mathcal{B}(D^0\eta)$ and $\mathcal{B}(D^0\pi^0)$. Note that in this case the δ' and θ phases compensate strongly for each other and $A_{D_s^+K^-}$ is small compared to $A_{D^0\eta}$ and $A_{D^0\pi^0}$.

For Fit2 of *DP* case, $\delta' (= 17.1^\circ)$ and $\theta (= -52.7^\circ)$ are opposite in sign. This favors the generation of $D^0\eta$ since the effects of δ' and θ add to each other. However, we would need a large θ phase to overcome the effect of δ' to generate

$D^0\pi^0$ mode i.e. to account for $|\delta| = |\delta_{1/2} - \delta_{3/2}| \sim 30^\circ$. Otherwise, we will have too small a $A_{D^0\pi^0}$ amplitude. Same as the previous case, a large phase of order 50° is needed to account for the strength of both the $D^0\pi^0$ and $D^0\eta$ modes. Inspecting the generation of $A_{D_s^+K^-}$, however, we see that the effects of δ' and θ now add to each other, and would generate too large a $\mathcal{B}(D_s^+K^-)$ that is already ruled out by data, hence the case is not plotted.

We also refrain from plotting the case for DV modes for the following reasons. First of all, because of relatively weaker rescattering, the a_2 effect is more prominent than in $D^{(*)}P$ case. Second, some discussion is already given in Sec. IV.B, where comparison is made between FSI and a_2 contributions. Decomposing into $A_{1/2}$ and $A_{3/2}$ amplitudes does not make the case clearer.

- [1] K. Abe *et al.* [BELLE Collaboration], Phys. Rev. Lett. **88**, 052002 (2002) [arXiv:hep-ex/0109021].
- [2] T. E. Coan *et al.* [CLEO Collaboration], Phys. Rev. Lett. **88**, 062001 (2002) [arXiv:hep-ex/0110055].
- [3] D. E. Groom *et al.* [Particle Data Group], Eur. Phys. J. C **15**, 1 (2000), and URL: <http://pdg.lbl.gov>.
- [4] M. Neubert and B. Stech, in *Heavy Flavours*, 2nd edition, ed. by A.J. Buras and M. Lindner (World Scientific, Singapore, 1998), p. 294 [hep-ph/9705292].
- [5] M. Beneke, G. Buchalla, M. Neubert and C. T. Sachrajda, Nucl. Phys. **B591**, 313 (2000) [hep-ph/0006124].
- [6] C. W. Bauer, D. Pirjol and I. W. Stewart, Phys. Rev. Lett. **87**, 201806 (2001) [hep-ph/0107002].
- [7] M. Neubert and A. A. Petrov, Phys. Lett. **B519**, 50 (2001) [hep-ph/0108103].
- [8] H.Y. Cheng, hep-ph/0108096, to be published in Phys. Rev. D.
- [9] M. Suzuki and L. Wolfenstein, Phys. Rev. D **60**, 074019 (1999) [hep-ph/9903477].
- [10] K. M. Watson, Phys. Rev. **88**, 1163 (1952).
- [11] Z.Z. Xing, hep-ph/0107257.
- [12] J.-M. Gerard and W.S. Hou, Phys. Rev. D **43**, 2909 (1991).
- [13] H. Georgi, Lie Algebras in Particle Physics, Addison-Wesley, 1982.
- [14] B. Grinstein and R. F. Lebed, Phys. Rev. D **53**, 6344 (1996) [hep-ph/9602218].
- [15] T. Feldmann, P. Kroll and B. Stech, Phys. Rev. D **58**, 114006 (1998) [hep-ph/9802409]; Phys. Lett. **B449**, 339 (1999) [hep-ph/9812269].
- [16] H.Y. Cheng and K.C. Yang, Phys. Rev. D **59**, 092004 (1999) [hep-ph/9811249].
- [17] H.Y. Cheng, C.Y. Cheung and C.W. Hwang, Phys. Rev. D **55**, 1559 (1997) [hep-ph/9607332].
- [18] J. F. Donoghue, E. Golowich, A. A. Petrov and J. M. Soares, Phys. Rev. Lett. **77**, 2178 (1996) [hep-ph/9604283].
- [19] K. Abe *et al.* [Belle Collaboration], BELLE-CONF-0125.
- [20] K. Abe *et al.* [Belle Collaboration], Phys. Rev. Lett. **87**, 111801 (2001) [hep-ex/0104051].
- [21] See the discussion by M. Suzuki, Proceedings of the Third International Conference on B Physics and CP Violation, Taipei, December 1999, ed. by H.Y. Cheng and W.S. Hou (World Scientific, Singapore, 2000), p. 259 [hep-ph/0001170].
- [22] X.G. He, W.S. Hou and K.C. Yang, Phys. Rev. Lett. **83**, 1100 (1999) [hep-ph/9902256]; W.S. Hou and K.C. Yang, Phys. Rev. D **61**, 073014 (2000) [hep-ph/9908202]; W.S. Hou, J. G. Smith and F. Wurthwein, hep-ex/9910014.
- [23] X.G. He, W.S. Hou and K.C. Yang, Phys. Rev. Lett. **81**, 5738 (1998) [arXiv:hep-ph/9809282].
- [24] An incomplete list is: A. F. Falk, A. L. Kagan, Y. Nir and A. A. Petrov, Phys. Rev. D **57**, 4290 (1998) [hep-ph/9712225]; D. Atwood and A. Soni, Phys. Rev. D **58**, 036005 (1998) [hep-ph/9712287]; B. Blok, M. Gronau and J. L. Rosner, Phys. Rev. Lett. **78**, 3999 (1997) [hep-ph/9701396]; N. G. Deshpande, X. G. He, W. S. Hou and S. Pakvasa, Phys. Rev. Lett. **82**, 2240 (1999) [hep-ph/9809329].
- [25] W.S. Hou and K.C. Yang, Phys. Rev. Lett. **84**, 4806 (2000) [hep-ph/9911528].